Iranian Journal of Fuzzy Systems

Volume 21, Number 6, (2024), pp. 101-126

Original paper

University of Sistan and Baluchestan

Parallel synchronization and a RBF neuro-fuzzy system to synchronization of chaotic systems

A. Mirzaei [1] and A. Nazemi [2]

[1,2] *Faculty of Mathematical Sciences, Shahrood University of Technology, Shahrood, Iran*

ali.mirzaei_1717@yahoo.com, nazemi20042003@gmail.com

Abstract

In this paper, an intelligent approach based on Radial Basis Function Neural Networks (RBFNNs) is used for synchronization problem between two chaotic systems. In this scheme, parallel systems have been first applied by converting the synchronization problem between two chaotic systems to synchronization problem between their parallel systems. By employing an active control strategy, an Infinite Horizon Optimal Control Problem (IHOCP) is constructed related to the obtained paralleled dynamical models. Using a suitable transformation, the IHOCP is then transformed into an equivalent finite-horizon one. According to Pontryagin Maximum Principle (PMP), the necessary optimality conditions for the finite horizon problem are examined in the form of two-point boundary value problems (TPBVPs). A fuzzy neural network approach that utilizes Radial Basis Functions (RBFs) as its activation functions for one of the hidden layers is established to approximate the solution of the TPBVP. By relying on the ability of RBFNN as function approximator, the trial solutions of variables are substituted in the TPBVP. The obtained algebraic nonlinear equations system is then reduced into an error function minimization problem. A learning scheme via center points of RBFs as training dataset and based on the Levenberg-Marquardt algorithm is employed as the optimizer to derive the adjustable parameters of trial solutions. Some various chaotic systems are synchronized based on numerical simulations to guarantee the capability of the proposed plan.

Keywords: Chaos synchronization, parallel synchronization, optimal control, fuzzy system, RBFNN, Levenberg-Marquardt algorithm.

1 Introduction

Chaos theory is a mathematical discipline that has found applications across various fields such as physics, economics, biology, and philosophy. This branch of study, exemplified by the Lorenz system developed by Lorenz [40], showcases how chaos manifests in natural phenomena. A deep comprehension of these systems has led to numerous advancements in areas like system control, modeling, and enhancing engineering implementations. A key characteristic of chaotic systems is their extreme sensitivity to initial conditions, suggesting that minor alterations in parameters can trigger significant shifts in system behavior.

Synchronization, which, in its simplest terms, means having identical dynamic behaviors. The idea of synchronization was initially introduced by Pecora and Carroll [8] and has garnered interest across numerous disciplines including physics [54], celestial mechanics [36], biology [21], and secure communications. In the realm of physics, synchronization has been utilized in electric power systems, digital electronics, and encryption systems. It also plays a role in medical fields; conditions like epilepsy [15] and Parkinson's disease [25] are associated with this phenomenon. Technologically, synchronization is crucial, especially in lasers. As the power of a laser increases, its stability typically diminishes. However, combining several low-power, stable lasers can create a high-power laser system. A significant challenge lies in ensuring these lasers remain synchronized to prevent destructive interference that could reduce power [27]. A

Corresponding Author: A. Nazemi
Received: May 2024; Revised: December 2024; Accepted: January 2025.
https://doi.org/10.22111/ijfs.2025.48808.8609

particularly intriguing aspect of synchronization is the synchronization of chaos, which describes a process where two chaotic systems align a specific characteristic of their motion to a common behavior through coupling. There are various types of synchronization that can occur among interacting systems, including identical synchronization [50], generalized synchronization [57], phase synchronization [55], anticipated synchronization [26, 64], lag synchronization [6], and amplitude envelope synchronization [22]. The occurrence of these synchronization types leads to the coupling of two or more chaotic systems.

In recent years, numerous control theory strategies have emerged to guarantee the coordination of a drive-response system. A majority of these techniques have effectively achieved synchronization between two chaotic systems, employing methods like encompassing nonlinear control methods [30], sliding mode control [71], linear matrix inequalities (LMI) [35], adaptive control methods [60], active control [66], and so on. Among them, active control approach is a powerful tool, which have been utilized to successfully deal with synchronization of chaotic systems by virtue of its flexibility, efficiency and simplicity in comparison with others synchronization methods. For more recent works and surveys of developments on the active control to synchronization of chaotic systems, one can see for instance [2, 16, 66, 69].

To apply an active control technique for synchronizing chaos, we view the system as follows:

$$\dot{X} = f(X), \quad X \in \mathbb{R}^n, \tag{1}$$

as a master system and a system

$$\dot{Y} = h(Y) + V(t), \quad Y \in \mathbb{R}^n,$$

as a slave system where $V(t) \in \mathbb{R}^n$ is an active control function which must be detected.

The paragraph describes a control system where an active control function $V(t)$ residing within the realm of $\mathbb{R}^n$ space, needs to be identified. This system operates under the principles of active control design to establish a suitable control function $V(t)$. The objective is to minimize the error $E(t) = Y - X$, which ideally should reduce to zero. To facilitate synchronization, the Lyapunov error function might be employed. When constructing a controller $V(t)$ for systems, various methodologies are available. For instance, Chen examined Lorenz and Lu systems, assuming typical feedback controls [12]. Alternatively, Huang broke down $f(X)$ and $h(Y)$ into linear and nonlinear forms, a strategy influenced by system parameters [30]. He then employed the Lyapunov error function $\mathcal{V}(E) = \frac{1}{2}E^T E$ to achieve synchronization, selecting the controller $V(t)$ to ensure $\frac{d}{dt}\mathcal{V}(E) < 0$. Despite the effectiveness of chaos synchronization techniques employing active control, their implementation presents challenges due to the complexity of active controllers and the selection of suitable control functions. In intricate systems, predicting the control function can be difficult, and synchronizing different systems with various active control functions can result in varying convergence error function rates.

To resolve these challenges in chaos synchronization, we propose a novel approach known as the parallel synchronization method. This method employs an active control technique to find a suitable condition for achieving active control in chaos synchronization scenarios. By leveraging this technique, we can formulate an optimal control problem to generate effective active control. The parallel synchronization method tackles the synchronization issues among various chaotic systems by harnessing the synchronization properties of their parallel counterparts. This method transforms the synchronization challenge into an optimal control problem, which ultimately helps identify the active control mechanism. The primary objective of optimal control is to devise control signals that not only meet specific physical constraints but also optimize a selected performance metric. Formulating an optimal control problem necessitates a model of the system, a definition of the performance index, the physical constraints on the system states, and the declaration of boundary conditions. In the parallel method, an appropriate cost functional is defined and minimized during the process of obtaining active control. This minimization leads to a reduction in synchronization error, thereby achieving near-zero synchronization error.

In the last several years, Artificial Intelligence (AI) has found widespread application across numerous domains [58]. The fundamental concept behind AI involves the fusion of human insights, specialized knowledge for specific tasks, computational intelligence, and processing capabilities. AI-based numerical methods have garnered significant interest due to their unique capacity to simplify complex nonlinear functions using straightforward models. One key benefit of these methods is that the solutions they produce are differentiable and expressed in closed analytic form.

Among AI plans, Artificial Neural Networks (ANNs) are computational models inspired by the structure and function of biological neural systems. They emulate the cognitive processes of the human brain, with mechanisms for both knowledge acquisition and storage. These networks consist of interconnected nodes, known as neurons, mirroring the synaptic connections within the nervous system. Each neuron's activity is governed by an activation function, which serves as a blueprint for potential processes occurring within actual brain cells. These functions enable the network to learn and generate desired outputs for various challenges. To comprehend the internal workings and performance of an

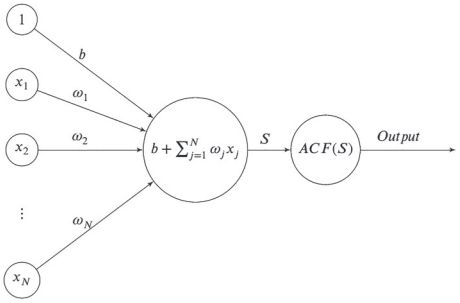


Figure 1: A simple NN framework.

ANN, one can visualize it as a directed graph. The vertices in this graph represent the neurons, and the edges symbolize the synapses connecting them. The nodes execute simple mathematical operations, such as activation functions, on the input data. This representation helps in understanding the intricate relationships between the components of the network and their collective effectiveness.

The numerical values assigned to the directed edges in a NN represent the information contained within those connections. These weights enable the network to learn and adjust over multiple iterations of inputting datasets. This weight update process, which varies depending on the type of inputs used, is known as learning. ANNs are classified based on their architecture into various types. Single-layer NNs consist solely of input and output neurons that are directly interconnected. In contrast, multilayer NNs incorporate additional neurons, known as bridge signals, which connect to at least one neuron from the preceding layer and another from the succeeding layer. These bridge signal neurons form what is referred to as a hidden layer. The configuration of hidden layers in multilayer NNs is influenced by factors such as the quantity of input signals, the number of input and output neurons, and the chosen learning strategies. An illustration of a basic NN design is depicted in Figure 1, where it represents a simple perceptron.

The rapid growth of ANN methods for solving various differential equations cannot be overlooked [33, 34, 73]. Various ANN frameworks exist to simulate dynamical systems, including RBFNNs [31, 41], Orthogonal NNs [53], and Deep NNs [45]. All these techniques rely on a nonlinear optimization approach. It's worth noting that numerous functions can serve as the basis in Orthogonal NNs. These functions can be classified into orthogonal and nonorthogonal categories. Orthogonal functions possess several desirable properties for approximating an unknown function, making them commonly used in this area. One significant group of orthogonal functions includes RBFs [9, 62]. RBFs are potent instruments for estimating approximations in high dimensions. They possess convergence and exponential order, and are not dependent on the network. Their simplicity and inherent universal approximation capabilities make them particularly useful in many fields, including data mining, pattern recognition, signal processing, time series prediction, and nonlinear system modeling and control [4, 7, 65].

RBFNNs have gained extensive attention due to their learning and generalization capabilities. Comparisons of RBFNNs with fuzzy systems, particularly rule-based systems, reveal intriguing similarities in terms of structure and learning algorithm. These NNs, hold significant importance within the realm of NNs. The primary characteristic of RBFNN is that the RBF serves as an activation function in the hidden layer, leading to numerous uses in function approximation. Recent studies suggest that RBFNNs demonstrate promising results when handling uncertain and ambiguous characteristics, creating a synergy effect between fuzzy logic and NNs. Researchers have recently explored the application of RBFNN's capabilities for addressing various problems in science and engineering. As some recent works, RBFNNs is introduced as an alternative approach, for the approximate solution of a Boundary Value Problem for second order quadratic Differential Equations, which arises in the numerical prediction of meteorological parameters [19]. A RBFNN algorithm is employed to solve the inverse Cauchy problems of the Laplace equation [49]. A sparse RBFNN method is proposed to solve elliptic partial differential equations with multiscale coefficients [67]. A Novel numerical method is suggested for solving ordinary differential equations using RBFNN with extreme learning machine algorithm [39]. A new approach based on RBF fuzzy systems is utilized for solving time delay fractional order optimal control problems. [47] An intelligent approach based on RBF fuzzy systems is employed for solving variable-order fractional delay differential algebraic equations [48].

Driven by past research, this paper explores the application of RBFNN for synchronization between two chaotic dynamical systems. In this approach, RBFNN solves TPBVP of the obtained optimal control problem via the active control scheme. To achieve this, we replace the trial solutions of state, co-state, and control variables within TPBVPs and discretize the time interval of the problem to convert the resulting system of nonlinear equations into a minimization problem of an error function. Lastly, we solve the resulting optimization problem to determine the adjustable parameters

of the trial solutions, using the Levenberg-Marquardt algorithm to calculate unknown parameters. It's worth noting that while there are numerous numerical methods for solving IHOCP related to synchronization problem of two chaotic systems, none have yet applied fuzzy logic systems with NNs. The primary contribution of this paper lies in the following:

- To solve the TPBVP problem, a computational method based on the RBF fuzzy system is proposed, which has not been investigated in the literature, to the best of our knowledge
- The solution of the IHOCP via the RBFNN is a smooth solution that can be easily used in any subsequent calculation. Most other techniques offer a discrete solution (for example, finite-difference methods [24]) or a solution with limited differentiability or dealing with finite meshes that significantly increase the computational cost (for example, embedding method [17, 18]), convergence proof difficulty of the generated series (for example, Adomian decosmposition method [59]) and difficulty in finding operational matrix (for example, spectral collocation methods [44]).
- The application of the RBFNN offers an effective resolution to TPBVP problems, demonstrating superior interpolation capabilities. This assertion is substantiated by comparing the results with the method outlined in [32], providing a clear validation of this approach.
- The proposed method significantly reduces the computational load compared to current techniques [13].

The paper is organized as follows. In Section 2, the concept of a parallel system for a chaotic system is introduced, where it can be done by by transforming the synchronization problem between two chaotic systems into the synchronization problem between their parallel systems. In Section 3, we give an appropriate condition to achieve an active control for chaos synchronization utilizing an optimal control strategy in infinite horizon state. In Section 4, we provide a brief introduction of RBFNN approach based on fuzzy systems and present a learning optimization algorithm for obtaining the adjustable parameters of the related optimal control problem. The way of updating the adjustable parameters using the Levenberg-Marquardt algorithm is addressed in Section 5. Numerical simulations are also given to validate the synchronization approach for each pair of the dynamical systems of Lorenz, Rossler and Liu in Section 6. Finally, this paper is ended with concluding remarks in Section 7.

2 Parallel synchronization method

Consider an ordinary differential equation (ODE) of the form

$$\begin{cases} \dot{X}(t) = f(X(t)), \\ X(0) = X_0, \end{cases} \tag{2}$$

where $f\colon \mathbb{R}^n \to \mathbb{R}^n$ is continuously differentiable in X.

Definition 2.1. [51] *Assume that f generates a flow $\Phi^t\colon \mathbb{R}^n \to \mathbb{R}^n$ such that $\Phi^t(X_0) = X(t)$, and consider the dynamical system $(f, \mathbb{R}^n, \Phi^t)$ derived from ODE (2). Let $f, g\colon \mathbb{R}^n \to \mathbb{R}^n$ be continuously differentiable functions defining the flows Φ^t and Ψ^t. Then, f and g are called topologically equivalent if there exists a homeomorphism L mapping the orbits of Φ^t onto the orbits of Ψ^t preserving the direction of time, i.e.,*

$$L(\Phi^t(X)) = \Psi^{\tau_Y(t)}Y,$$

where $Y = L(X)$ and $\Psi^{\tau_Y(t)}$ is increasing in t.

Definition 2.2. [51] *A closed invariant set $\Lambda \subseteq R^n$ is called an attracting set if there is some positively invariant neighborhood $\tilde{U}$ of Λ such that for every $t \geq 0$ we have*

$$\bigcap_{t\geq 0} \Phi^t(\tilde{U}) = \Lambda.$$

Definition 2.3. [51] *An attractor is a topologically transitive attracting set. Suppose that $\Lambda \subseteq \mathbb{R}^n$ is an attractor. Then Λ is called a strange attractor or a chaotic attractor if it is chaotic.*

Definition 2.4. [32] *Let $f, g\colon \mathbb{R}^n \to \mathbb{R}^n$ be continuously differentiable functions defining the flows $\Phi(t, X) = \Phi^t(X)$ and $\Psi(t, X) = \Psi^t(X)$, respectively. Then the dynamical system $\Psi(t, X)$ is said to be a parallel system of the dynamical system $\Phi(t, x)$ if for all $X \in \mathbb{R}^n$ and all $t \in \mathbb{R}$ one has that $s\Phi(t, X) = \Psi(t, sX)$, for some $s \in R^+$. This implies that the two dynamical systems generated by f and g are topologically equivalent by the homeomorphism $L\colon \mathbb{R}^n \to \mathbb{R}^n$ defined by $L(X) = sX$. Indeed,*

$$L(\Phi^t(X)) = s\Phi^t(X) = \Psi(sX) = \Psi^t(L(X)). \tag{3}$$

Moreover, L preserves the direction of time, because $\tau_Y(t) = t$, where $Y = L(X)$.

In order to synchronize chaotic systems using active control function, we employ a parallel synchronization method. The proposed schemes guide us to construct on optimal control problem which achieves the active control.

We first consider the master system (1), and then take a slave system given by

$$\dot{Y} = h(Y) + D_1V_1(t),\ Y \in \mathbb{R}^n, \tag{4}$$

where $D_1 \in \mathbb{R}^{n\times n}$ and $V_1(t) \in \mathbb{R}^n$ is an active control function. The main goal is to find the active control function such that the slave system can pursue the master system. We define error synchronization and error dynamic between two systems (1) and (4) is respectively given by

$$\begin{cases} E_1(t) = Y - X, \\ \dot{E}_1(t) = h(Y) - f(X) + D_1V_1(t). \end{cases} \tag{5}$$

By selecting an appropriate controller function $V_1(t)$, the defined error functions converge to zero. To apply the parallel synchronization method, we choose a parallel system

$$\dot{Z} = g(Z),\ Z \in \mathbb{R}^n, \tag{6}$$

of (1) as a master parallel system and a system as

$$\dot{W} = k(W) + D_2V_2(t),\ W \in \mathbb{R}^n,\ D_2 \in \mathbb{R}^{n\times n}, \tag{7}$$

as a slave parallel system of (4) (defined by a constant $s_1 \in \mathbb{R}^+$) with the active controller $V_2 \in \mathbb{R}^n$, where system

$$\dot{W} = k(W),\ W \in \mathbb{R}^n, \tag{8}$$

is also a parallel system (defined by a constant $s_2 \in \mathbb{R}^+$) for the system

$$\dot{Y} = h(Y),\ Y \in \mathbb{R}^n. \tag{9}$$

Error synchronization and error dynamic between two systems (6) and (7) are respectively defined by

$$\begin{cases} E_2(t) = W - Z = s_2Y - s_1X, \\ \dot{E}_2(t) = k(W) - g(Z) + D_2V_2(t). \end{cases} \tag{10}$$

3 An optimal control problem

The synchronization problem between two systems (1) and (4) can be transformed to an optimal control problem. For this purpose, we define two combined systems, the first is as

$$\begin{pmatrix} \dot{X} \\ \dot{Z} \end{pmatrix} = \begin{pmatrix} f(X) \\ g(Z) \end{pmatrix}, \tag{11}$$

as a (main) master system, and other one is given by

$$\begin{pmatrix} \dot{Y} \\ \dot{W} \end{pmatrix} = \begin{pmatrix} h(Y) + D_1V_1(t) \\ k(W) + D_2V_2(t) \end{pmatrix}, \tag{12}$$

as a (main) slave system.

Theorem 3.1. [32] *The combined system* (11) *is synchronized with* (12) *if and only if the two master chaotic systems* (1) *and* (6) *are synchronized with the systems given by* (4) *and* (7)*, respectively.*

Now we transform the synchronization problem between systems (11) and (12) to an optimal control problem. By solving the optimal control problem, it is shown that (11) is synchronized to (12). To reach this goal, we consider the master chaotic systems (1) and (6) in the form

$$\begin{cases} \dot{X} = \tilde{C}_1 X + \tilde{f}(X), \\ \dot{Z} = \hat{D}_1 Z + \hat{g}(Z), \end{cases} \tag{13}$$

and (4) and (7) in the form

$$\begin{cases} \dot{Y} = \tilde{C}_2 Y + \tilde{h}(Y) + D_1 V_1(t), \\ \dot{W} = \hat{D}_2 W + \hat{k}(W) + D_2 V_2(t). \end{cases} \tag{14}$$

Utilizing (5),(10),(13) and (14), we obtain

$$\begin{cases} \dot{E}_1(t) = C_1 E_1(t) + f_1(E_1, E_2) + D_1 V_1(t), \\ \dot{E}_2(t) = C_2 E_2(t) + f_2(E_1, E_2) + D_2 V_2(t), \end{cases}$$

which in a compact form is

$$\dot{E}(t) = CE(t) + DV(t) + f(E), \tag{15}$$

where

$$E(t) = \begin{pmatrix} E_1(t) \\ E_2(t) \end{pmatrix}, \quad C = \begin{pmatrix} C_1 & O \\ O & C_2 \end{pmatrix}, \quad D = \begin{pmatrix} D_1 & O \\ O & D_2 \end{pmatrix}, \quad f(E) = \begin{pmatrix} f_1(E_1, E_2) \\ f_2(E_1, E_2) \end{pmatrix}, \quad V(t) = \begin{pmatrix} V_1(t) \\ V_2(t) \end{pmatrix}.$$

and O is the zero matrix.

Remark 3.2. *We use the following norms for any function* $\eta : [0, \infty) \to \mathbb{R}^n$ *in* $L_2([0, \infty))$*,*

$$\|\eta(t)\|_2 = \left(\sum_{i=1}^{n} |\eta_i(t)|^2 \right)^{\frac{1}{2}}, \qquad t \geq 0,$$

$$\|\eta(.)\|_{L_2} = \left(\int_0^\infty \|\eta(t)\|_2^2 \mathrm{d}t \right)^{\frac{1}{2}},$$

where n *is a given finite number,* $\eta(t) = (\eta_1(t), \eta_2(t), \ldots, \eta_n(t))^T$ *and* $\eta_i(t) : [0, \infty) \to \mathbb{R}$*,* $i = 1, 2, \ldots, n$*.*

Definition 3.3. (**Synchronization problem**): *The controller* $V(t), t \geq 0$ *can be designed to ensure synchronization between systems* (11) *and* (12)*, if the corresponding output* $E(.)$ *of system* (15) *satisfies* $\lim_{t\to\infty} \|E(t)\|_2^2 = 0$*.*

Now we focus on the error system (15) as the continues-state system and $V(t)$ as the active control function and suggest an error function related to (15) as follows

$$I(E(.), V(.)) = \int_0^\infty (E^T(t)\tilde{Q}E(t) + V^T(t)\tilde{R}V(t))dt, \tag{16}$$

where $\tilde{Q} \in \mathbb{R}^{2n\times 2n}$ is a positive semi-definite matrix and $\tilde{R} \in \mathbb{R}^{2n\times 2n}$ is a positive definite matrix. In order to synchronize between systems (11) and (12), we must find a control function $V(t) : [0, \infty) \to B \subseteq \mathbb{R}$ by solving the following IHOCP

$$\text{minimize} \quad I(E(.), V(.)) \tag{17}$$

$$\text{subject to} \quad \begin{cases} \dot{E}(t) = CE(t) + DV(t) + f(E), \\ E(t_0) = E_0. \end{cases} \tag{18}$$

The following assumptions hold throughout this paper:

i) $E(t) \in A \subseteq \mathbb{R}^{2n}$ and $V(t) \in B \subseteq \mathbb{R}^{2n}$ are, respectively, the values of the phase vector of system (18) and of the control vector at time $t \geq 0$, A is a nonempty compact rectangular box in $\mathbb{R}^{2n}$, B is a nonempty compact rectangular box in $\mathbb{R}^{2n}$, and $E_0 \in \mathbb{R}^{2n}$ is a given initial state of the system (18).

ii) It is easy to verify that the right hand side of the dynamical system (18) and the integrand in (16) are continuously differentiable in $E(t)$.

iii) The class of admissible controls for system (18) is the set of all (Lebesgue) measurable functions $V : [0, \infty) \to B$.

iv) An admissible trajectory of system (18) corresponding to an admissible control $V(t)$ is defined to be a (Carathéodory) solution $E(t)$ of the differential equation (18), which is defined on $t \in [0, \infty)$, satisfies the initial condition in (18) and takes values in A.

v) We assume that for every admissible control V there exists an admissible trajectory E corresponding to V and the (Lebesgue) integral in (16) converges absolutely.

Definition 3.4. *An admissible pair $(E^*(.), V^*(.))$ is an optimal solution of problem (17)-(18) if*

$$I(E(t), V(t))\, dt \geq I(E^*(t), V^*(t))dt,$$

for any admissible pair $(E(t)^T, V(t)^T)^T$.

We now examine that by solving IHOCP (17) and (18), the system (11) is synchronized with (12).

Theorem 3.5. *If $I(E^*(.), V^*(.))$ be an optimal solution of IHOCP* (17) *and* (18) *with $I(E^*(.), V^*(.)) < \infty$, then controller $V^*(t), t \geq 0$ synchronizes between systems* (11) *and* (12)*, i.e. $\lim_{t\to\infty} \|E^*(t)\|^2 = 0$.*

Proof. From assumption i), it yields that the optimal pair $(E^{*\top}(t), V^{*\top}(t))$ of system (18) is bounded. Therefore, there exists an increasing sequence $\{t_n\}$ with $\lim_{n\to\infty} t_n = \infty$ and a limit point $(\hat{E}^\top, \hat{V}^\top)^\top$, such that $\lim_{n\to\infty} E^*(t_n) = \hat{E}$ and $\lim_{n\to\infty} V^*(t_n) = \hat{V}$.

We now show that $\lim_{t\to\infty} \|E^*(t)\|^2 = 0$. If it does not hold, that is

$$\lim_{t\to\infty} \|E^*(t)\|^2 = \|\hat{E}\|^2 > 0. \tag{19}$$

Define

$$D(E, V) = E^\top(t)\tilde{Q}E(t) + V^\top(t)\tilde{R}V(t).$$

It is easy to verify that $D(\hat{E}, \hat{V}) > 0$ (by positive semi-definiteness of $\tilde{Q}$, positive definiteness of $\tilde{R}$ and using (19)). It is also clear that $D(E^*(t), V^*(t))$ is continuous with respect to E^* and V^* respectively. Thus, there exist $\varepsilon > 0$, $q > 0$ and a ε neighborhood of $(\hat{E}^\top, \hat{V}^\top)^\top$ as

$$B((\hat{E}, \hat{V}), \varepsilon) = \{(E^*(t)^\top, V^*(t)^\top)^\top \ \ \|E^* - \hat{E}\| + \|V^* - \hat{V}\| \leq \varepsilon\},$$

such that $D(E^*(t), V^*(t)) > q$, for all $(E^*(t)^\top, V^*(t)^\top)^\top \in B((\hat{E}, \hat{V}), \varepsilon)$. Noting that $\lim_{n\to\infty} E^*(t_n) = \hat{E}$ and $\lim_{n\to\infty} V^*(t_n) = \hat{V}$; thus there exists a positive integer N, such that for all $n \geq N$, $\|E^*(t_n) - \hat{E}\| \leq \frac{1}{4}\varepsilon$, $\|V^*(t_n) - \hat{V}\| \leq \frac{1}{4}\varepsilon$.

From the boundedness of $(E^*(t)^\top, V^*(t)^\top)^\top$ we have $\dot{E}^*$ and $\dot{V}^*$ are also bounded, denoted by M. Considering $t \in \left[t_n - \frac{\varepsilon}{8M}, t_n + \frac{\varepsilon}{8M}\right]$, $n \geq N$ we have

$$\begin{aligned}
\|E^*(t) - \hat{E}\| + \|V^*(t) - \hat{V}\| \leq & \|E^*(t) - E^*(t_n)\| + \|V^*(t) - V^*(t_n)\| + \|E^*(t_n) - \hat{E}\| + \|V^*(t_n) - \hat{V}\| \\
= & \|\dot{E}^*(\xi_1)\| \times |t - t_n| + \|\dot{V}^*(\xi_2)\| \times |t - t_n| + \|E^*(t_n) - \hat{E}\| + \|V^*(t_n) - \hat{V}\| \\
\leq & 2M|t - t_n| + \frac{\varepsilon}{2} \leq \varepsilon.
\end{aligned}$$

That is, for all $t \in \left[t_n - \frac{\varepsilon}{8M}, t_n + \frac{\varepsilon}{8M}\right]$, $n \geq N$, $(E^*(t)^\top, V^*(t)^\top)^\top \in B((\hat{E}, \hat{V}), \varepsilon)$. Therefore, $D(E^*(t), V^*(t)) > q$, for all $t \in \left[t_n - \frac{\varepsilon}{8M}, t_n + \frac{\varepsilon}{8M}\right]$, $n \geq N$. Since $\lim_{n\to\infty} t_n = \infty$, and the Lebesgue measure of set $\cup_{n\geq N} \left[t_n - \frac{\varepsilon}{8M}, t_n + \frac{\varepsilon}{8M}\right]$ is infinite, then we have

$$I(E^*(.), V^*(.)) = \int_0^\infty D(E^*(t), V^*(t))\, dt = \infty. \tag{20}$$

Thus $I(E^*(.), V^*(.))$ is not finite which is a contradiction. Thus we have $\lim_{t\to\infty} \|E^*(t)\|^2 = 0$. This completes the proof. □

We now convert infinite horizon problem (17) and (18) to a finite horizon one by the following time transformation

$$t = \frac{\tau}{(1-\tau)}, \quad t \in [0,\infty), \quad \tau \in [0,1). \tag{21}$$

Thus, (17) and (18) is equivalently replaced by

$$\text{minimize} \qquad \int_{[0,1)} (e^T(\tau)\tilde{Q}e(\tau) + v^T(\tau)\tilde{R}v(\tau))\frac{d\tau}{(1-\tau)^2} \tag{22}$$

subject to

$$\dot{e}(\tau) = \frac{1}{(1-\tau)^2}(Ce(\tau) + Dv(\tau) + f(e(\tau))), \tag{23}$$

$$e(0) = E_0, \tag{24}$$

where

$$\begin{cases} e(\tau) = E(\frac{\tau}{1-\tau}), \\ v(\tau) = V(\frac{\tau}{1-\tau}). \end{cases}$$

The Hamiltonian for the optimal control problem (22)-(24) can be stated by

$$H(\tau, e(\tau), v(\tau), p(\tau)) = \frac{1}{(1-\tau)^2}\left((e^T(\tau)\tilde{Q}e(\tau) + v^T(\tau)\tilde{R}v(\tau)) + p(\tau).(Ce(\tau) + Dv(\tau) + f(e(\tau)))\right),$$

where $p \in \mathbb{R}^{2n}$ is the costate vector. According to the PMP, if $e(\tau), v(\tau)$ and $p(\tau)$ are, respectively, the optimal values of the state, costate and control of (22)-(24), they must satisfy the following necessary conditions:

$$\begin{cases} \dfrac{\partial H(\tau, e, v, p)}{\partial e} = -\dot{p}(\tau), \\ \dfrac{\partial H(\tau, e, v, p)}{\partial p} = \dot{e}(\tau), \\ \dfrac{\partial H(\tau, e, v, p)}{\partial v} = 0, \\ e(0) = E_0, \\ \lim_{\tau \to 1^-} p(\tau) = 0, \end{cases} \tag{25}$$

for all $\tau \in [0,1)$. It is follows that (25) yields a system of TPBVPs, which can be solved via numerical methods or other existing methods. In the next section, we try to use the ability of fuzzy systems NNs in function approximation to solve (25).

4 RBFNN approach

A fuzzy system consists of four principal parts whose basic configuration is depicted in Figure 2,

a) a fuzzifier, which is a map from crisp points into fuzzy sets in the input space,

b) fuzzy rule base, a set of fuzzy rules that perform the fuzzy system. The fuzzy rules have the following form:

$$\begin{cases} R_j \ (j\text{th rule}): & \text{If } x_1 \text{ is } A_1^j \text{ and } x_2 \text{ is } A_2^j \text{ and} \cdots \text{and } x_n \text{ is } A_n^j, \\ & \text{Then } z \text{ is } B^j, \end{cases} \tag{26}$$

where n is the number of input variables, $x_i, (i = 1, \cdots, n)$ and z are the input and output variables, respectively and A_i^j and B^j are linguistic terms characterized by fuzzy membership functions $\mu_{A_i^j}(x_i)$ and $\mu_{B^j}(z)$, respectively,

c) inference engine, which determines a mapping based on fuzzy logic operations on fuzzy rule base,

d) a defuzzifier, which is a map from fuzzy sets into crisp points in the output space.

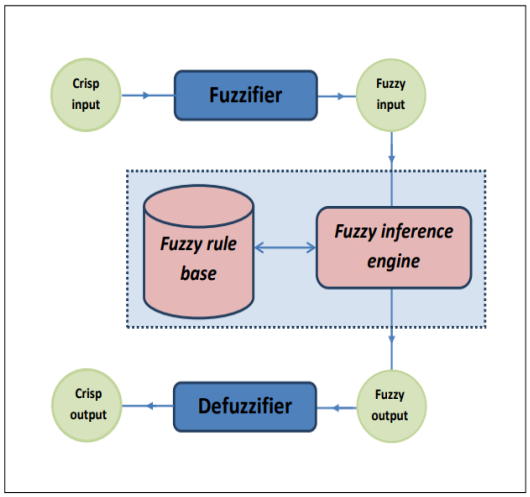


Figure 2: Basic configuration of fuzzy systems.

A subset of the fuzzy systems of Figure 2 with singleton fuzzifier, product inference, centroid defuzzifier, and Gaussian membership function consists of all functions of the form

$$\tilde{f}(x) = \frac{\sum_{j=1}^{m} w_j (\prod_{i=1}^{n} \mu_{A_i^j}(x_i))}{\sum_{j=1}^{m} (\prod_{i=1}^{n} \mu_{A_i^j}(x_i))}, \tag{27}$$

where $\tilde{f} : U \subset \mathbb{R}^n \longrightarrow \mathbb{R}$, $x = (x_1, x_2, \ldots, x_n)^\top \in U$, w_j is the weight related to each fuzzy rule, $\mu_{A_i^j}(x_i)$ are the fuzzy membership functions corresponding to each input x_i, m is the number of fuzzy rules and n is the number of input variables. Essentially, the w_j values play a key role in calculating the final output of the fuzzy system by weighting the membership of inputs in the fuzzy functions. The stated fuzzy system is known as Takagi-Sugeno (T-S) system.

Wang and Mendel in [68] proved that fuzzy systems (27) can uniformly approximate any nonlinear continuous function under a compact set to any degree of accuracy. This property can be expressed by means of the following theorem:

Theorem 4.1. (Universal Approximation Theorem)[68] *For any given real continuous $\tilde{h}(x)$ on the compact set $U \subset \mathbb{R}^n$ and arbitrary $\varepsilon > 0$, there exists $\tilde{f}(x) \in Y$ (Y is the set of all the functions (27)) such that*

$$\sup_{x \in U} |\tilde{f}(x) - \tilde{h}(x)| < \varepsilon. \tag{28}$$

In this paper we consider a fuzzy system with an input variable $\tau \in [0, 1)$ and output variable $\tilde{f}(\tau) \in \mathbb{R}$ which can be implemented by the following function:

$$\tilde{f}(\tau) = \sum_{i=1}^{M} d_i \frac{\mu_i}{\sum_{i=1}^{M} \mu_i} = W^\top \Phi, \tag{29}$$

where $W = [w_1, w_2, \ldots, w_M]^\top$, $\Phi = [\phi_1, \phi_2, \ldots, \phi_M]^\top$, $\phi_i = \dfrac{\mu_i}{\sum_{i=1}^{M} \mu_i}$ and μ_i $i = 1, 2, \ldots, M$ are Gaussian membership functions in the following form:

$$\mu_i = \exp(-\frac{1}{2}(\frac{\tau - a_i}{\sigma_i})^2), \tag{30}$$

where a_i and σ_i are the mean values and the standard deviations of the membership distributions, assigned respectively as follows:

$$a_i = (i-1)\frac{\tau_f}{M-1}, \tag{31}$$

$$\sigma_i = \frac{\tau_f}{M-1}, \tag{32}$$

where $M > 1$ is the numbers of fuzzy rules.

Remark 4.2. *Throughout this paper, we assume τ_f tends to 1 from left side, i.e. $\tau_f \to 1^-$.*

Remark 4.3. *The Gaussian function is a nonlinear function in $C^\infty[0,1)$. Hence this makes the approximate solution* (28)-(30) *smooth, continuous and differentiable in $C^\infty[0,1)$ in order to save the properties of the exact solution.*

Remark 4.4. *From* (32) *, it is easy to find out that the standard deviations σ_i will be forced to be zero with infinite numbers of membership functions, i.e., $\lim_{M\to\infty} \sigma_i = 0$. Therefore, when M approaches to ∞ membership function in* (30) *degenerate into the singleton case from the Gaussian case.*

Based on Theorem 4.1, it is shown that any continuous function $\tilde{h}(\tau)$ for $\tau \in [0,1)$ can be approximated by the suggested fuzzy system $\tilde{f}(\tau)$ with a sufficient number of fuzzy rules. Hence, due to the universal approximation property of the fuzzy systems, the discussed fuzzy system (27) can be utilized for approximating the unknown solutions of the TPBVPs (25). Now, with the aim of designing a RBFNN based on the fuzzy system (27), we provide a fundamental representation of an orthogonal NN with one input layer, an orthogonal layer as the hidden layer that can be considered as a functional expansion block, an output layer that has a single node, and a topology like that in Figure 3, in which $\phi_i(\tau)$s are the RBFs on $[0,1)$ and w_is is are called weights of the network. In order to enhance the accuracy and prevent the approximation of the derivative, the identity function is selected as the activation function of the output neuron [23]. So, by considering the network as in Figure 3, the outputs of this fuzzy NN related to (25) to state variables $e(\tau)$, Lagrangian multipliers $p(\tau)$ and control functions $v(\tau)$ are as follows:

$$\begin{cases} N_e(\tau, w^e) = W_e^\top \Phi, \\ N_p(\tau, w^p) = W_p^\top \Phi, \\ N_v(\tau, w^v) = W_v^\top \Phi, \end{cases} \tag{33}$$

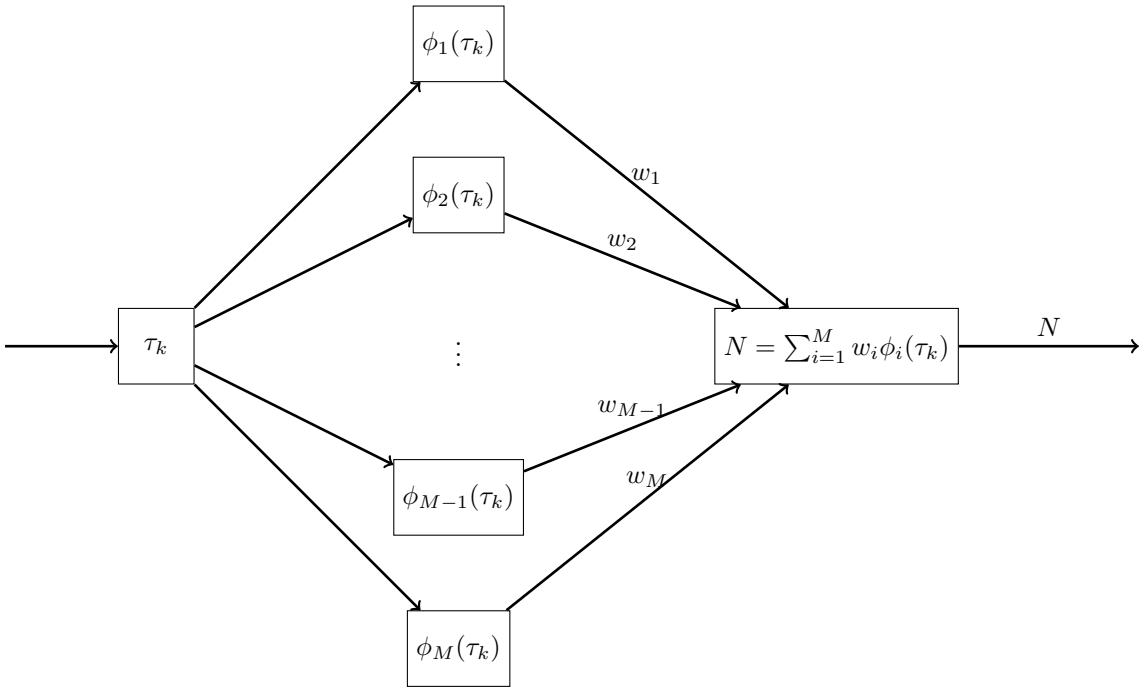


Figure 3: The topology of RBFNN model.

The remaining vital steps to be taken are satisfying the optimality conditions set and training the network in such a way that it approximates the solution on the whole problem domain accurately and efficiently. In order to solve (25) by the proposed fuzzy NN system (33), first, it is necessary to approximate $(e(\tau)^\top, p(\tau)^\top, v(\tau)^\top)^\top$ based on the fuzzy network schemes. Then by constructing a suitable cost function and minimizing it, and, finally, training the fuzzy network such that the approximations of $(e(\tau)^\top, p(\tau)^\top, v(\tau)^\top)^\top$ satisfy (25). Utilizing these facts and using (33), the trial fuzzy approximator solutions may be written as the sum of two terms in the following forms:

$$\begin{cases} e_T(\tau) = e(0) + \tau N_e(\tau, w^e), \\ p_T(\tau) = (\tau_f - \tau) N_p(\tau, w^p), \\ v_T(\tau) = N_v(\tau, w^v), \end{cases} \tag{34}$$

where the first term satisfies initial or boundary conditions and contains no adjustable parameters. The second term makes no contribution to initial or boundary conditions but this is employed by a fuzzy system whose weights are adjusted to minimize the error function. The number of fuzzy rules can be different for each fuzzy approximator.

Fuzzy approximator solutions in (34) should be satisfied in system (25), we then get

$$\begin{cases} \dot{e}_T(\tau) = \dfrac{\partial H_T}{\partial p_T}, \\ \dot{p}_T(\tau) = -\dfrac{\partial H_T}{\partial e_T}, \\ 0 = \dfrac{\partial H_T}{\partial v_T}, \end{cases} \tag{35}$$

where

$$H_T = H(e_T, p_T, v_T, \tau).$$

The next step of this approach is finding the best training dataset on which the fuzzy network is taught to find the solution with the minimum error. To achieve this goal, the roots of RBFs are used not only they maximize the convergence rate, but also they are well-scattered on the problem domain and will approximate the satisfactory solution on the interval rather than only on the neighborhood of training points. Let us assume $\tilde{D} = \{\tau_1 = a_1, \tau_2 = a_2, \ldots, \tau_s = a_s\}$ as the training data set denoted in (30). The following cost function is formed in a way that $\zeta = (e(\tau)^\top, p(\tau)^\top, v(\tau)^\top)^\top$ will be the solution of (25):

$$E(\zeta, \vartheta) = \frac{1}{2} \sum_{i=1}^{3} \sum_{k=1}^{s} \{E_i(\tau_k, \vartheta)\}, \tag{36}$$

where $\vartheta = (w^{e\top}, w^{p\top}, w^{v\top})^\top$ and

$$\begin{cases} E_1(\tau_k, \vartheta) = \left[\dot{e}_T(\tau) - \dfrac{\partial H_T}{\partial p_T}\right]^2_{|\tau=\tau_k}, \\ E_2(\tau_k, \vartheta) = \left[\dot{p}_T(\tau) + \dfrac{\partial H_T}{\partial e_T}\right]^2_{|\tau=\tau_k}, \\ E_3(\tau_k, \vartheta) = \left[\dfrac{\partial H_T}{\partial v_T}\right]^2_{|\tau=\tau_k}. \end{cases} \tag{37}$$

For leading ϑ^* to become an optimal solution of (35), the cost function should be minimized. Hence, the problem reduces to the following nonlinear least square problem:

$$\text{argmin}_\vartheta \; E(\zeta, \vartheta). \tag{38}$$

In the next section, we illustrate the approach used for solving this nonlinear least square problem. For this purpose, the Levenberg-Marquardt algorithm is established, which is used to minimize the cost function value in (38).

Remark 4.5. *Note that in the suggested approach, when parameters of the original system are changed, the active control function also change. Thus, the proposed chaotic systems works online. It is clear that the desired active control function related to the changed system must be determined by the presented RBF neural network scheme, where weights w^v are adjusted to minimize the error function. Thus, the achieved RBF neural network is also works on-line.*

5 Levenberg-Marquardt algorithm

Among different problems appearing in the nonlinear system of equations and nonlinear optimization problems, finding a proper solution to the nonlinear least-square problems is extremely well-known among scientist. For minimizing a

vector function, $\| \tilde{g}(x) \|$, where $\tilde{g} : \mathbb{R}^n \longrightarrow \mathbb{R}^m$, and $m \geq n$ with respect to a predefined $x = (x_1, x_2, \ldots, x_n)^\top$, where $x^* \in \mathbb{R}^n$ is found in a way that

$$\tilde{G}(x) = \frac{1}{2}\tilde{g}^\top(x).\tilde{g}(x), \tag{39}$$

in which

$$x^* = \text{argmin}_x\{\tilde{G}(x)\}.$$

Various schemes have been studied for solving this nonlinear least square model up to now; however, here, a more competent approach is proposed. The preliminary definitions are stated as follows:

Since $\tilde{G} : \mathbb{R}^n \longrightarrow \mathbb{R}$, its first-order derivative is defined with the aid of gradient vector as

$$s(x) = \frac{\partial \tilde{G}}{\partial x}(x) = J(x)^\top.\tilde{g}(x),$$

where the Jacobian matrix $J(x)$ is defined as follows:

$$J(x)_{ij} = \frac{\partial \tilde{g}_i}{\partial x_j}(x).$$

The second-order derivative of $\tilde{G}(x)$, which indicates its Hessian matrix H, is as the following form:

$$H = J^\top(x).J(x) + \sum_{i=1}^{m} \tilde{g}_i(x)\tilde{g}_i^{''}(x).$$

Using Taylor expansion $\tilde{g}$ on $x + h$ can be approximated as

$$\tilde{g}(x + h) = \tilde{g}(x) + J(x)h + o(\| h \|^2).$$

Solving nonlinear equation systems is one of many valuable applications of nonlinear least square models by studying the following nonlinear system:

$$\tilde{g}(x) = 0, \qquad \text{where} \qquad \tilde{g} : \mathbb{R}^n \longrightarrow \mathbb{R}^n,$$

and $x = (x_1, x_2, \ldots, x_n)^\top$. Detecting the solution to this problem with the help of classic Newton-Rophson scheme leads us to solve the linear system stated in (41) per each iteration as is stated by Newton's iterative method:

$$x_{n+1} = x_n - J(x_n)^{-1}\tilde{G}(x_n), \tag{40}$$

$$\begin{cases} J(x_n)h_n = \tilde{G}(x_n), \\ x_{n+1} = x_n + h_n. \end{cases} \tag{41}$$

It can be verified that for an invertible (nonsingular) $J(x^k)$, the procedure converges quadratically. The other challenge in this method is the distance between x_k and x^*; further distances may cause the scheme to fail.

One feasible operation to be taken in a conflict with these issues is global minimization of the function $\tilde{G}(x) = \frac{1}{2} \| \tilde{g}(x) \|^2$. The Newton method updating process in (41) can be substituted with the following equation, taking into account that $\tilde{G}(x^*) = 0$ and $\tilde{G}(x) > 0$ if $\tilde{g}(x^*) = 0$:

$$x_{n+1} = x_n + a_n h_n,$$

a_n indicates the step-size that can be found using line search method applied to $\tilde{G}(x_n + ah_n)$. h_n is the descent direction. h_n can be calculated using gradient method or Gauss-Newton method. A refinement for h_n have been calculated by a method suggested by Levenberg (1994) and later Marquardt (1963) through a damped plan as

$$(J_n^\top J_n + \mu I)h_n = s_n, \qquad \text{where} \qquad s = J^\top k,$$

where I is a diagonal matrix and $\mu \geq 0$ depicts the damping parameter to provide the algorithm with a proper $h_i n$ that is in a descent direction. When μ is a small value, we have

$$(J_n^\top J_n)h_n = J^\top \tilde{g},$$

which is a proper step in the final stages of iteration when x is close to x^*. However, we achieve a short step in steepest descent direction, if μ is a large value, because $h_n = -\frac{1}{\mu}s_n$, which is a good step in the final stages of iteration when x is close to x^*. Moreover, it is important to mention that the initial vector x_0 is a random vector whose elements are random numbers between -0.2 and 0.2. For the convergence analysis of the Levenberg-Marquardt algorithm, the reader may refer to More [46].

6 Numerical examples

In order to verify the chaos synchronization via applying the parallel synchronization, a RBFNN approach, two examples are presented. In the first example, the synchronization between the Rossler [56] and Lorenz [40] systems is addressed. In the second example, we test the reliability of the parallel synchronization method by synchronizing between the Rossler and Liu[38] systems.

Lorenz system is defined by

$$\begin{cases} \dot{X}_1 = \alpha(X_2 - X_1), \\ \dot{X}_2 = \gamma X_1 - X_2 - X_1 X_3, \\ \dot{X}_3 = -\beta X_3 + X_1 X_2. \end{cases} \tag{42}$$

With $\alpha = 10$, $\beta = \frac{8}{3}$ and $\gamma = 28$, (42) is Lorenz chaotic system.

Rossler system is defined by

$$\begin{cases} \dot{X}_1 = -X_2 - X_3, \\ \dot{X}_2 = X_1 + aX_2, \\ \dot{X}_3 = bX_1 - cX_3 + X_1 X_3. \end{cases} \tag{43}$$

When $a = 0.32$, $b = 0.3$ and $c = 4.8$, (43) is Rossler chaotic system.

Liu system is defined by

$$\begin{cases} \dot{X}_1 = -aX_1 - eX_2^2, \\ \dot{X}_2 = bX_2 - kX_1 X_3, \\ \dot{X}_3 = -cX_3 + mX_1 X_2. \end{cases} \tag{44}$$

With $a = 1$, $e = 1$, $b = 2.5$, $k = 4$, $c = 5$ and $m = 4$, (44) is Liu chaotic system.

Example 6.1. (Synchronization between the Rossler and Lorenz systems)

Consider Rossler chaotic system (43) *as a master system and system*

$$\begin{cases} \dot{X}_1 = \alpha(X_2 - X_1) + V_1, \\ \dot{X}_2 = \gamma X_1 - X_2 - X_1 X_3 + V_2, \\ \dot{X}_3 = -\beta X_3 + X_1 X_2 + V_3, \end{cases} \tag{45}$$

as a slave system. The parallel system of Rossler system (43) *with constant* $s = 1$ *is defined by*

$$\begin{cases} \dot{Z}_1 = -Z_2 - Z_3, \\ \dot{Z}_2 = Z_1 + 0.32 Z_2, \\ \dot{Z}_3 = 0.3 Z_1 - 4.8 Z_3 + Z_1 Z_3. \end{cases}$$

The parallel system of Lorenz system (42) *with constant* $s = \frac{1}{2}$ *is defined as*

$$\begin{cases} \dot{W}_1 = 10(W_2 - W_1), \\ \dot{W}_2 = 28 W_1 - W_2 - 2 W_1 W_3, \\ \dot{W}_3 = -\dfrac{8}{3} W_3 + 2 W_1 W_2. \end{cases}$$

In order to achieve synchronization, we employ the parallel synchronization method. For this goal, consider the combined system

$$\begin{cases} \dot{X}_1 = -X_2 - X_3, \\ \dot{X}_2 = X_1 + 0.32 X_2, \\ \dot{X}_3 = 0.3 X_1 - 4.8 X_3 + X_1 X_3, \\ \dot{X}_4 = -X_5 - X_6, \\ \dot{X}_5 = X_4 + 0.32 X_5, \\ \dot{X}_6 = 0.3 X_4 - 4.8 X_6 + X_4 X_6, \end{cases} \tag{46}$$

as the (main) master system and the combined system

$$\begin{cases} \dot{Y_1} = 10(Y_2 - Y_1) + V_1, \\ \dot{Y_2} = 28Y_1 - Y_2 - Y_1Y_3 + V_2, \\ \dot{Y_3} = -\frac{8}{3}Y_3 + 2Y_1Y_2 + V_3, \\ \dot{Y_4} = 10(Y_5 - Y_4) + V_4, \\ \dot{Y_5} = 28Y_4 - Y_5 - 2Y_4Y_6 + V_5, \\ \dot{Y_6} = -\frac{8}{3}Y_6 + 2Y_4Y_5 + V_6, \end{cases} \tag{47}$$

as the (main) slave system. The initial values for (46) *are taken as* $X_1(0) = X_2(0) = X_4(0)X_5(0) = 0.5$ *and* $X_3(0) = X_6(0) = 1.5$. *The initial values for* (47) *are taken as* $Y_1(0) = Y_2(0) = Y_3(0) = 1$, *and* $Y_4(0) = Y_5(0) = Y_6(0) = 2$. *The error functions are given as*

$$E_i = Y_i - X_i, i = 1, 2, ..., 6. \tag{48}$$

In order to synchronization between (46) *and* (47), *we have to solve the following IHOCP as*

$$\text{minimize} \quad I(E(.), V(.)) = \frac{1}{2}\int_0^{\infty} (E^2(t) + V^2(t))dt \tag{49}$$

$$\text{subject to} \quad \begin{cases} \dot{E_1} = -20E_1 + 21E_2 + E_3 + 20E_4 - 22E_5 - 2E_6 + V_1, \\ \dot{E_2} = 55E_1 - 2.32E_2 - 54E_4 + 2.64E_5 - 4(E_1 - E_4)(E_3 - E_6) + V_2, \\ \dot{E_3} = -0.3E_1 - 8.15E_3 + 0.6E_4 - 64.15E_6 + 4(E_1 - E_4)(E_2 - E_5) - (E_1 - 2E_4)(E_3 - 2E_6) + V_3, \\ \dot{E_4} = -10E_1 + 11E_2 + E_3 + 10E_4 - 12E_5 - 2E_6 + \frac{1}{2}V_4, \\ \dot{E_5} = 27E_1 - 1.32E_2 - 26E_4 + 1.64E_5 - 2(E_1 - E_4)(E_3 - E_6) + \frac{1}{2}V_5, \\ \dot{E_6} = -0.3E_1 + 32.15E_3 + 0.6E_4 - 104.15E_6 + 2(E_1 - E_4)(E_2 - E_5) - (E_1 - 2E_4)(E_3 - 2E_6) + \frac{1}{2}V_6, \\ E_0 = (0.5.0.5, -0.5, 1.5, 1.5, 0.5)^{\top}. \end{cases} \tag{50}$$

The related finite horizon of (49) *and* (50) *is*

$$\text{minimize} \quad I(e(.), v(.)) = \frac{1}{2}\int_{[0,1)} (e^2(\tau) + v^2(\tau))\frac{1}{(1-\tau)^2}d\tau, \tag{51}$$

$$\text{subject to} \quad \begin{cases} \dot{e_1} = -20e_1 + 21e_2 + e_3 + 20e_4 - 22e_5 - 2e_6 + v_1, \\ \dot{e_2} = 55e_1 - 2.32e_2 - 54e_4 + 2.64e_5 - 4(e_1 - e_4)(e_3 - e_6) + v_2, \\ \dot{e_3} = -0.3e_1 - 8.15e_3 + 0.6e_4 - 64.15e_6 + 4(e_1 - e_4)(e_2 - e_5) - (e_1 - 2e_4)(e_3 - 2e_6) + v_3, \\ \dot{e_4} = -10e_1 + 11e_2 + e_3 + 10e_4 - 12e_5 - 2e_6 + \frac{1}{2}v_4, \\ \dot{e_5} = 27e_1 - 1.32e_2 - 26e_4 + 1.64e_5 - 2(e_1 - e_4)(e_3 - e_6) + \frac{1}{2}v_5, \\ \dot{e_6} = -0.3e_1 + 32.15e_3 + 0.6e_4 - 104.15e_6 + 2(e_1 - e_4)(e_2 - e_5) - (e_1 - 2e_4)(e_3 - 2e_6) + \frac{1}{2}v_6, \\ e_0 = (0.5.0.5, -0.5, 1.5, 1.5, 0.5)^{\top}. \end{cases} \tag{52}$$

According to (25)*, the necessary optimality conditions are as follows:*

$$\begin{cases}
\dot{e}_1 + 20e_1 - 21e_2 - e_3 - 20e_4 + 22e_5 + 2e_6 - v_1 = 0,\\
\dot{e}_2 - 55e_1 + 2.32e_2 + 54e_4 - 2.64e_5 + 4(e_1 + e_4)(e_3 + e_6) - v_2 = 0,\\
\dot{e}_3 + 0.3e_1 + 8.15e_3 - 0.6e_4 + 64.15e_6 - 4e_1e_2 - 4e_1e_5 + 4e_4e_2 - e_4e_5 + e_1e_3 - 2e_1e_6 - 2e_4e_3\\
+4e_4e_6 - v_3 = 0,\\
\dot{e}_4 + 10e_1 - 11e_2 - e_3 - 10e_4 + 12e_5 + 2e_6 - \frac{1}{2}v_4 = 0,\\
\dot{e}_5 - 27e_1 + 1.32e_2 + 26e_4 - 1.64e_5 + 2e_1e_3 - 2e_1e_6 - 2e_4e_3 + 2e_4e_6 - 1/2v_5 = 0,\\
\dot{e}_6 + 0.3e_1 - 32.15e_3 - 0.6e_4 + 104.15e_6 - 2e_1e_2 + 2e_1e_5 + 2e_4e_2 - 2e_4e_5 + e_1e_3 - 2e_1e_6 - 2e_4e_3\\
+4e_4e_6 - \frac{1}{2}v_6 = 0,\\
\dot{p}_1 + e_1 - 20p_1 + 55p_2 - 4p_2e_3 + 4p_2e_6 - 0.3p_3 + p_3e_2 - 4p_3e_5 - p_3e_3 + p_3e_6 - 10p_4 + 27p_5,\\
-2p_5e_3 + 2p_5e_6 - 0.3p_6 + 2p_6e_2 - 2p_6e_5 - p_6e_3 + 2p_6e_6 = 0,\\
\dot{p}_2 + e_2 + 21p_1 - 2.32p_2 + 4p_3e_1 - 4p_3e_4 + p_4 - 1.32p_5 + 2p_6e_1 - 2p_6e_4 = 0,\\
\dot{p}_3 + e_3 + p_1 - 4p_2e_1 + 4p_2e_4 - 8.15p_3 - p_3e_1 + 2p_3e_4 + p_4 - 2p_5e_1 + 2p_5e_4 + 32.15p_6,\\
-p_6e_1 + 2p_6e_4 = 0,\\
\dot{p}_4 + e_4 + 20p_1 - 54p_2 + 4p_2e_3 - 4p_2e_6 + 0.6p_3 - 4p_3e_2 + 4p_3e_5 + 2p_3e_3 - 4p_3e_6 + 10p_4,\\
-26p_5 + 2p_5e_3 - 2p_5e_6 + 0.6p_6 - 2p_6e_2 + 2p_6e_5 + 2p_6e_3 - 4p_6e_6 = 0,\\
\dot{p}_5 + e_5 - 22p_1 + 2.64p_2 - 4p_3e_1 + 4p_3e_4 - 0 - 12p_4 + 1.64p_5 - 2p_6e_1 + 2p_6e_4 = 0,\\
\dot{p}_6 + e_6 - 2p_1 + 4p_2e_1 - 4p_2e_4 - 64.15p_3 + 2p_3e_1 - 4p_3e_4 - 2p_4 + 2p_5e_1 - 2p_5e_4 - 104.15p_6,\\
+2p_6e_1 - 4p_6e_4 = 0,\\
v_1 + p_1 = 0,\\
v_2 + p_2 = 0,\\
v_3 + p_3 = 0,\\
v_4 + 1/2p_4 = 0,\\
v_5 + 1/2p_5 = 0,\\
v_6 + 1/2p_6 = 0.
\end{cases}$$

The trial approximator solutions can be considered as follows:

$$\begin{cases}
e_{1T} = 0.5 + \tau N_{e_1},\\
e_{2T} = 0.5 + \tau N_{e_2},\\
e_{3T} = -0.5 + \tau N_{e_3},\\
e_{4T} = 1.5 + \tau N_{e_4},\\
e_{5T} = 1.5 + \tau N_{e_5},\\
e_{6T} = 0.5 + \tau N_{e_6},\\
p_{1T} = (-\tau + \tau_f) N_{p_1},\\
p_{2T} = (-\tau + \tau_f) N_{p_2},\\
p_{3T} = (-\tau + \tau_f) N_{p_3},\\
p_{4T} = (-\tau + \tau_f) N_{p_4},\\
p_{5T} = (-\tau + \tau_f) N_{p_5},\\
p_{6T} = (-\tau + \tau_f) N_{p_6},\\
v_{1T} = N_{v_1},\\
v_{2T} = N_{v_2},\\
v_{3T} = N_{v_3},\\
v_{4T} = N_{v_4},\\
v_{5T} = N_{v_5},\\
v_{6T} = N_{v_6}.
\end{cases}$$

All simulation results are depicted to validate the accuracy of the method with $s = 20$ *and* $M = 10$*. For example, Figure 4 depicts the active control functions* $v_i(.), i = 1, ..., 6$*. Figure 5 shows that the error functions* $e_i(.), i = 1, ..., 6$ *approaches to zero. Thus, systems* (46) *and* (47) *are synchronized. Consequently, based on Theorem* (3.5)*, synchronization between the Rossler and Lorenz systems with an active control function is happened.*

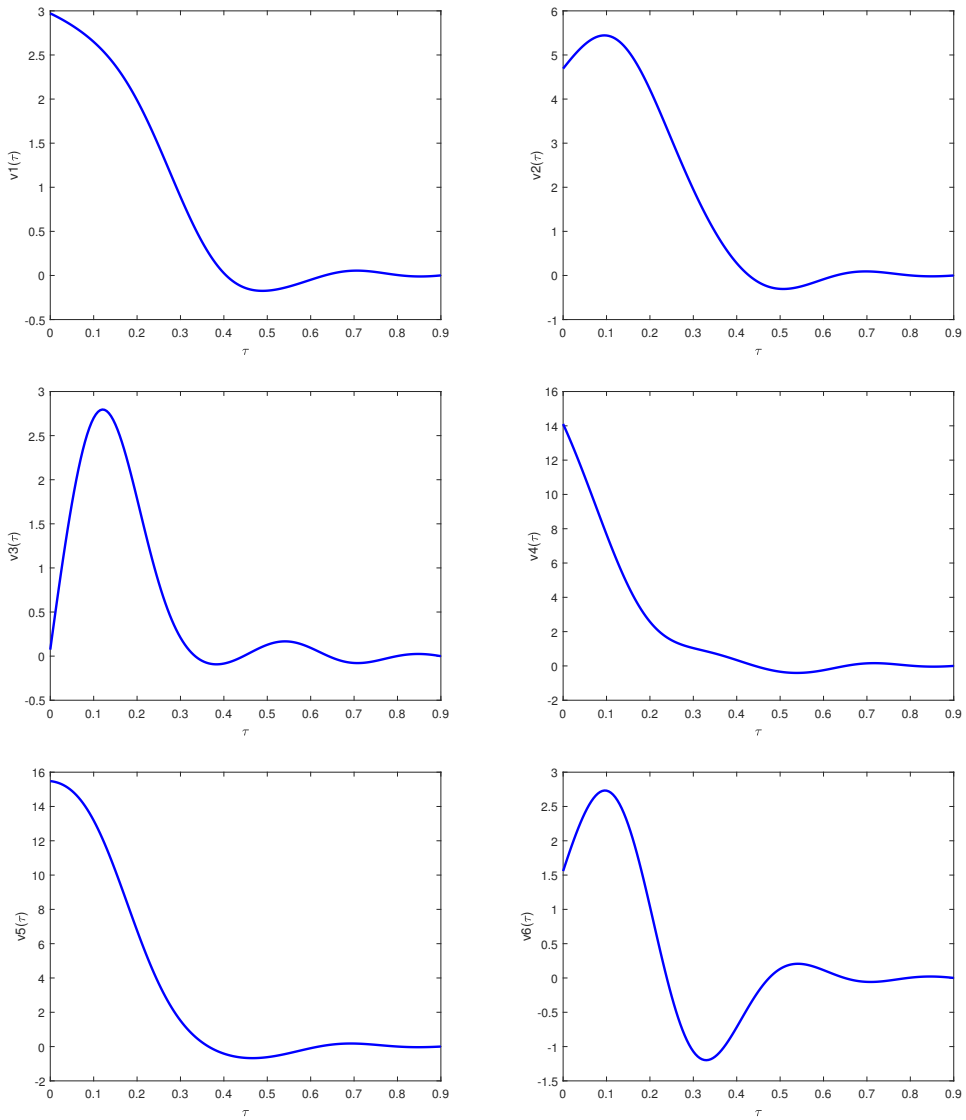


Figure 4: Active control functions $v_i(.), i = 1, ..., 6$ to synchronize between (46) and (47).

Example 6.2. (Synchronization between the Liu and Rossler systems)
Consider Rossler chaotic system (43) *as a master system and system*

$$\begin{cases} \dot{X}_1 = -aX_1 - eX_2^2 + V_1, \\ \dot{X}_2 = bX_2 - kX_1X_3 + V_2, \\ \dot{X}_3 = -cX_3 + mX_1X_2 + V_3, \end{cases} \tag{53}$$

as a slave system. The parallel system of the Rossler system (43) *with constant* $s = 3$ *is*

$$\begin{cases} \dot{Z}_1 = -Z_2 - Z_3, \\ \dot{Z}_2 = Z_1 + 0.32Z_2, \\ \dot{Z}_3 = 0.32Z_1 - 4.8Z_3 + \dfrac{1}{3}Z_1Z_3. \end{cases} \tag{54}$$

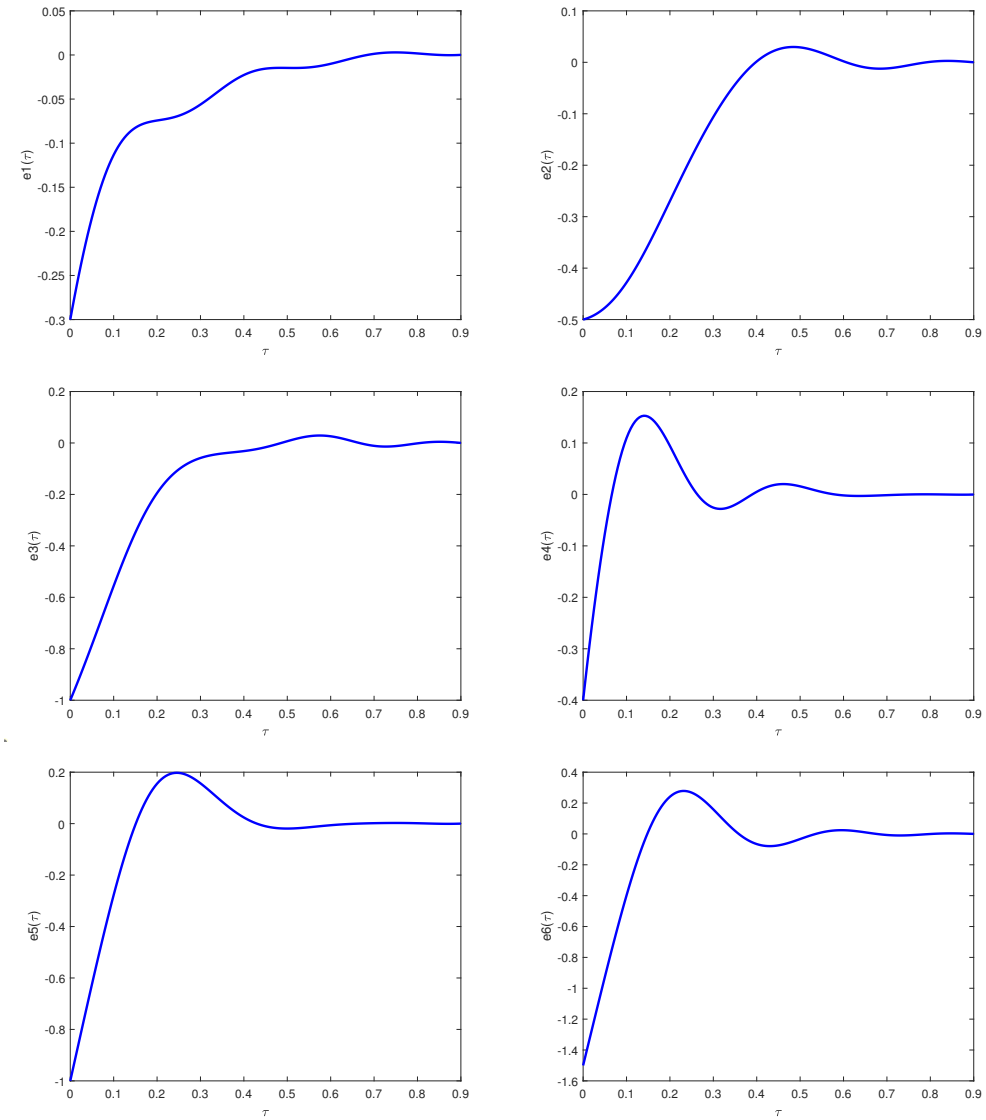


Figure 5: Error functions $e_i(.), i = 1, ..., 6$.

As a parallel system of Liu system (44) *with* $s = 2$ *we get*

$$\begin{cases} \dot{W}_1 = -W_1 - \dfrac{1}{2}W_2^2, \\ \dot{W}_2 = 2.5W_2 - 2W_1W_3, \\ \dot{W}_3 = -5W_3 + 2W_1W_2. \end{cases} \tag{55}$$

The combined master system is

$$\begin{cases} \dot{X}_1 = -X_2 - X_3, \\ \dot{X}_2 = X_1 + 0.32X_2, \\ \dot{X}_3 = 0.3X_1 - 4.8X_3 + X_1X_3, \\ \dot{X}_4 = -X_5 - X_6, \\ \dot{X}_5 = X_4 + 0.32X_5, \\ \dot{X}_6 = 0.3X_4 - 4.8X_6 + \dfrac{1}{3}X_4X_6. \end{cases} \tag{56}$$

The combined slave system is

$$\begin{cases} \dot{Y_1} = -Y_1 - Y_2^2 + V_1, \\ \dot{Y_2} = 2.5Y_2 - 4Y_1Y_3 + V_2, \\ \dot{Y_3} = -5Y_3 + 4Y_1Y_2 + V_3, \\ \dot{Y_4} = -Y_4 - \dfrac{1}{2}Y_5^2 + V_4, \\ \dot{Y_5} = 2.5Y_5 - 2Y_4Y_6 + V_5, \\ \dot{Y_6} = -5Y_6 + 2Y_4Y_5 + V_6. \end{cases} \tag{57}$$

The initial values are selected as $X_1(0) = X_2(0) = X_4(0) = X_5(0) = 0.5$, $X_3(0) = X_6(0) = 1.5$ *and* $Y_1(0) = 0.2$, $Y_2(0) = Y_5(0) = 0$, $Y_3(0) = 0.5$, $Y_4(0) = 0.6$, $Y_6(0) = 1.5$. *The error functions are given by*

$$E_i = Y_i - X_i, i = 1, 2, ..., 6. \tag{58}$$

In order to synchronization between (56) *and* (57), *we must solve the following IHOCP as*

$$\text{minimize} \quad I(E(.), V(.)) = \frac{1}{2}\int_0^{\infty} (E^2(t) + V^2(t))dt, \tag{59}$$

$$\text{subject to} \quad \begin{cases} \dot{E_1} = -3E_1 + 2E_2 + 2E_3 + E_4 - E_5 - E_6 - (E_5 - 3E_2)^2 + V_1, \\ \dot{E_2} = -2E_1 + 6.86E_2 + E_4 + 2.18E_5 - 4(E_4 - 3E_1)(E_6 - 3E_3) + V_2, \\ \dot{E_3} = -0.6E_1 - 5.4E_3 + 0.3E_4 + 0.2E_6 - (E_4 - 2E_1)(E_6 - 2E_3) - 4(E_4 - 3E_1) \\ (E_5 - 3E_2) + V_3, \\ \dot{E_4} = -6E_1 + 6E_2 + 4E_3 - 3E_5 + 2E_6 + 2E_4 - 2(E_5 - 2E_2)^2 + V_4, \\ \dot{E_5} = -6E_1 + 13.08E_2 + 3E_4 - 4.4E_5 - 8(E_4 - 3E_1)(E_6 - 3E_3) + V_5, \\ \dot{E_6} = -1.8E_1 - 1.2E_3 + 0.9E_4 - 4.4E_6 - 3(E_5 - 2E_2)(E_6 - 2E_3) + 8(E_4 - 3E_1) \\ (E_5 - 3E_2) + V_6, \\ E_0 = (-0.3, -0.5, -1, -0.4, -1, -1.5)^{\top}. \end{cases} \tag{60}$$

The related finite horizon problem of (59) *and* (60) *is*

$$\text{minimize} \quad I(e(.), v(.)) = \frac{1}{2}\int_{[0,1)} (e^2(\tau) + v^2(\tau))\frac{1}{(1-\tau)^2}d\tau, \tag{61}$$

$$\text{subject to} \quad \begin{cases} \dot{e_1} = -3e_1 + 2e_2 + 2e_3 + e_4 - e_5 - e_6 - (e_5 - 3e_2)^2 + v_1, \\ \dot{e_2} = -2e_1 + 6.86e_2 + e_4 + 2.18e_5 - 4(e_4 - 3e_1)(e_6 - 3e_3) + v_2, \\ \dot{e_3} = -0.6e_1 - 5.4e_3 + 0.3e_4 + 0.2e_6 - (e_4 - 2e_1)(e_6 - 2e_3) - 4(e_4 - 3e_1) \\ (e_5 - 3e_2) + v_3, \\ \dot{e_4} = -6e_1 + 6e_2 + 4e_3 - 3e_5 + 2e_6 + 2e_4 - 2(e_5 - 2e_2)^2 + v_4, \\ \dot{e_5} = -6e_1 + 13.08e_2 + 3e_4 - 4.4e_5 - 8(e_4 - 3e_1)(e_6 - 3e_3) + v_5, \\ \dot{e_6} = -1.8e_1 - 1.2e_3 + 0.9e_4 - 4.4e_6 - 3(e_5 - 2e_2)(e_6 - 2e_3) + 8(e_4 - 3e_1) \\ (e_5 - 3e_2) + v_6, \\ e_0 = (-0.3, -0.5, -1, -0.4, -1, -1.5)^{\top}. \end{cases} \tag{62}$$

According to (25)*, the necessary optimality conditions is*

$$
\begin{cases}
\dot{e}_1(t) + 3e_1(t) - 2e_2(t) - 2e_3(t) - e_4(t) + e_5(t) + e_6(t) + (e_5(t) - 3e_2(t))^2 - v_1(t) = 0, \\
\dot{e}_2(t) + 2e_1(t) - 6.89e_2(t) - e_4(t) + 2.184e_5(t) + 4(e_4(t) - 3e_1(t))(e_6(t) - 3e_3(t)) - v_2(t) = 0, \\
\dot{e}_3(t) + 0.6e_1(t) + 5.4e_3(t) - 0.3e_4(t) - 0.2e_6(t) + (e_4(t) - 2e_1(t))(e_6(t) - 2e_3(t)) + 4(e_4(t) \\
-3e_1(t))(e_5(t) - 3e_2(t)) - v_3(t) = 0, \\
\dot{e}_4(t) + 6e_1(t) - 6e_2(t) - 4e_3(t) + 3e_5(t) - 2e_6(t) - 2e_4(t) + 2(e_5(t) - 3e_e(t))^2 - v_4(t) = 0, \\
\dot{e}_5(t) + 6e_1(t) - 13.08e_2(t) - 3e_4(t) + 4.04e_5(t) + 8(e_4(t) - 3e_1(t))(e_6(t) - 3e_3) - v_5(t) = 0 \\
\dot{e}_6(t) + 1.8e_1(t) + 1.2e_3(t) - 0.9e_4(t) + 4.4e_6(t) + 3(e_5(t) - 2e_2(t))(e_6(t) - 2e_3(t)) - 8(e_4(t) - 3e_1(t)), \\
(e_5(t) - 3e_2(t)) - v_6(t) = 0, \\
\dot{p}_1(t) + e_1(t) - 3p_1(t) - 2p_2(t) + 12p_2(t)e_6(t) - 36p_2(t)e_3(t) - 0.6p_3(t) + 2p_3(t)e_6(t) - 4p_3(t)e_3(t) \\
+12p_3(t)e_5(t) - 36p_3(t)e_2(t) - 6p_4(t) - 6p_5(t) + 24p_5(t)e_6(t) - 72p_5(t)e_3(t) - 1.8p_6(t) \\
-24p_6(t)e_5(t) + 72p_6(t)e_2(t) = 0, \\
\dot{p}_2(t) + e_2(t) + 2p_1(t) + 6p_1(t)e_5(t) - 18p_1(t)e_2(t) + 6.86p_2 + 12e_4(t)p_3(t) - 36p_3(t)e_1(t) + 6p_4(t) \\
+12p_4(t)e_5(t) - 36p_4(t)e_2(t) + 13.08p_5(t) + 6p_6(t)e_6(t) - 12p_6(t)e_3(t) - 24p_6(t)e_4(t) \\
+72p_6(t)e_1(t) = 0, \\
\dot{p}_3 + e_3(t) + 2p_1(t) + 12p_2(t)e_4(t) - 36p_2(t)e_1(t) - 5.4p_3(t) + 2p_3(t)e_4(t) - 4p_3(t)e_1(t) + 4p_4(t) \\
+24p_5(t)e_4(t) - 72p_5(t)e_1(t) - 1.2p_6(t) + 6p_6(t)e_5(t) - 12p_6(t)e_2(t) = 0, \\
\dot{p}_4 + e_4(t) + p_1(t) + p_2(t) - 4p_2(t)e_6(t) + 12p_2(t)e_3(t) + 0.3p_3(t) - p_3(t)e_6(t) + 2p_3(t)e_3(t) \\
-4p_3(t)e_5(t) + 12p_3(t)e_2(t) + 2p_4(t) + 3p_5(t) - 8p_5(t)e_6(t) + 24p_5(t)e_3(t) + 0.9p_6(t) + 8p_6(t)e_5(t) \\
-24p_6(t)e_2(t) = 0, \\
\dot{p}_5 + e_5(t) - p_1(t) - 2p_1(t)e_5(t) + 6p_1(t)e_2(t) - 2.18p_2(t) - 4p_3(t)e_4(t) + 12p_3(t)e_1(t) - 3p_4(t) \\
-4p_4(t)e_5(t) + 12p_4(t)e_2(t) - 4.04p_5(t) - 3p_6(t)e_6(t) + 6p_6(t)e_3(t) + 8p_6(t)e_4(t) - 24p_6(t)e_1(t) = 0, \\
\dot{p}_6 + e_6(t) - p_1(t) - 4p_2(t)e_4(t) + 12p_2(t)e_1(t) + 0.2p_3(t) - p_3(t)e_4(t) + 2p_3(t)e_1(t) + 2p_4(t) \\
-8p_5(t)e_4(t) + 24p_5(t)e_1(t) - 4.4p_6(t) - 3p_6(t)e_5(t) + 6p_6(t)e_2(t) = 0, \\
v_1 + p_1 = 0, \\
v_2 + p_2 = 0, \\
v_3 + p_3 = 0, \\
v_4 + p_4 = 0, \\
v_5 + p_5 = 0, \\
v_6 + p_6 = 0.
\end{cases}
$$

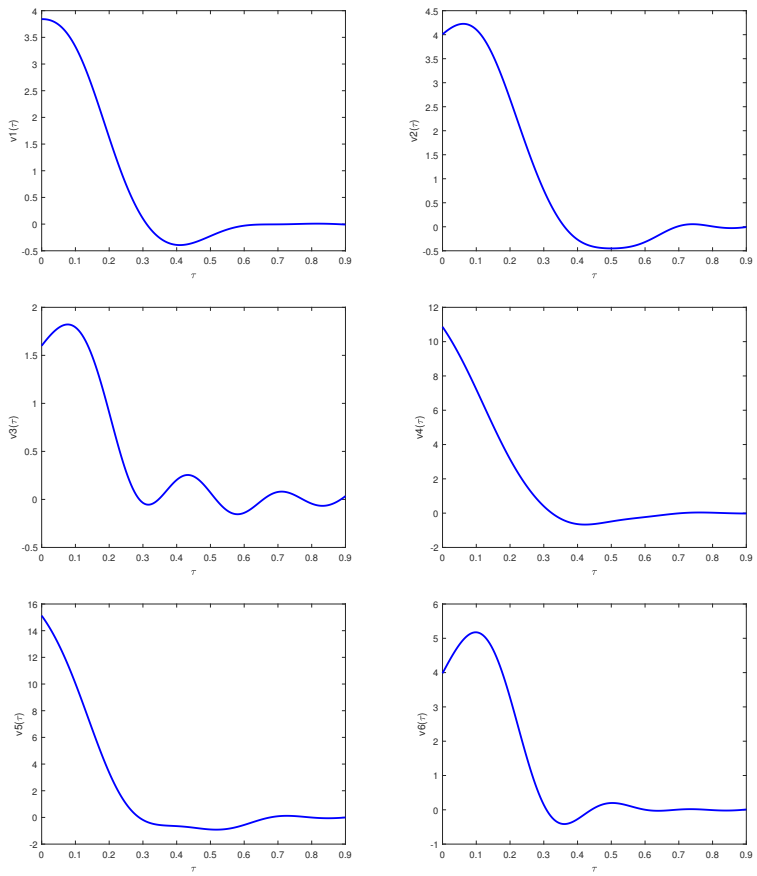


Figure 6: Active control functions $v_i(.), i = 1, ..., 6$ to synchronize between (56) and (57).

The trial approximator solutions can be constructed as follows:

$$\begin{cases} e_{1T} = -0.3 + \tau N_{e_1}, \\ e_{2T} = -0.5 + \tau N_{e_{12}}, \\ e_{3T} = -1 + \tau N_{e_3}, \\ e_{4T} = -0.4 + \tau N_{e_4}, \\ e_{5T} = -1 + \tau N_{e_5}, \\ e_{6T} = -1.5 + \tau N_{e_6}, \\ p_{1T} = (-\tau + \tau_f) N_{p_1}, \\ p_{2T} = (-\tau + \tau_f) N_{p_2}, \\ p_{3T} = (-\tau + \tau_f) N_{p_3}, \\ p_{4T} = (-\tau + \tau_f) N_{p_4}, \\ p_{5T} = (-\tau + \tau_f) N_{p_5}, \\ p_{6T} = (-\tau + \tau_f) N_{p_6}, \\ v_{1T} = N_{v_1}, \\ v_{2T} = N_{v_2}, \\ v_{3T} = N_{v_3}, \\ v_{4T} = N_{v_4}, \\ v_{5T} = N_{v_5}, \\ v_{6T} = N_{v_6}. \end{cases}$$

All simulation results are depicted to validate the accuracy of the method with with $s = 20$ *and* $M = 10$. *For*

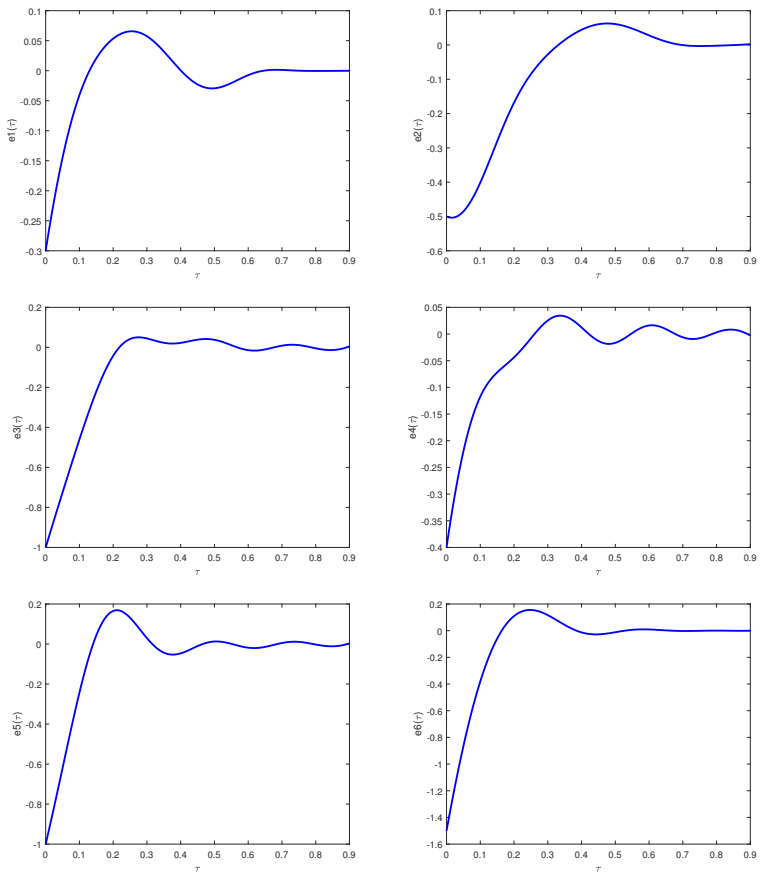


Figure 7: Error functions $e_i(.), i = 1, ..., 6$.

example, Figure 6 depicts the active control functions $v_i(.), i = 1, ..., 6$. *Figure 7 shows that the error functions* $e_i(.), i = 1, ...,6$ *approaches to zero. Thus, systems* (56) *and* (57) *are synchronized. Consequently, based on Theorem* (3.5), *synchronization between the Liu and Rossler systems with an active control function is made.*

7 Conclusion

This study introduces a new approach based on optimal control strategy in infinite horizon state to synchronizing chaotic systems known as the parallel synchronization method. A RBFNN based on fuzzy logic systems are also employed to solve the obtained TPBVPs. By converting the synchronization issue between two chaotic systems into one involving their parallel counterparts, this method offers a way to achieve active control for chaos synchronization. The synchronization challenge is transformed into an optimal control problem, which helps to identify the optimal control strategy. The advantage of this active control is its superior convergence error function rate and ability to drive the dynamic system towards a desired state or optimize a performance metric, ensuring the quickest transition from an arbitrary initial state to a specific final state. It also minimizes the overall energy consumption during synchronization. The main advantage of the mentioned method is that it is not very complicated, and the accuracy of the approximation solution can be increased using more training points in the interval $[0, 1)$. To implement the optimal control problem, a suitable performance index is defined by minimizing the quadratic performance, followed by deriving the control function. The study demonstrates that the synchronization error converges to zero by solving TPBVPs. Numerical results support the efficacy and reliability of the parallel synchronization technique. The method is versatile and can be employed for various synchronization types such as anti-synchronization, adaptive synchronization, lag synchronization, and even for synchronizing fractional order chaotic systems. Moreover, it holds potential for chaos control of chaotic systems.

Acknowledgments

Data availability Enquiries about data availability should be directed to the authors.

Declarations

Conflict of interest Both of the authors declare that they have no conflict of interest.

Ethical approval This article does not contain any studies with animals performed by any of the authors.

References

[1] M. A. Abdelkawy, A. Z. M. Amin, A. H. Bhrawy, J. A. T. Machado, A. M. Lopes, *Jacobi collocation approximation for solving multi-dimensional Volterra integral equations*, International Journal of Nonlinear Sciences and Numerical Simulation, **18**(5) (2017), 411-425. https://doi.org/10.1515/ijnsns-2016-0160

[2] M. T. Akter, A. Tarammim, S. Hussen, *Chaos control and synchronization of modified Lorenz system using active control and backstepping scheme*, Waves in Random and Complex Media, (2023). https://doi.org/10.1080/17455030.2023.2205529

[3] G. V. Badalyan, *Generalization of Legendre polynomials and some of their applications*, Russian, Armenian Summary, **9**(3a) (1956), 22. https://doi.org/10.1007/978-3-0348-8685-7-13

[4] F. Behloul, B. P. F. Lelieveldt, A. Boudraa, J. H. C. Reiber, *Optimal design of radial basis function neural networks for fuzzy-rule extraction in high dimensional data*, Pattern Recognition, **35** (2002), 659-675. https://doi.org/10.1016/S0031-3203(01)00033-4

[5] A. H. Bhrawy, *A Jacobi spectral collocation method for solving multi-dimensional nonlinear fractional sub-diffusion equations*, Numerical Algorithms, **73**(1) (2016), 91-113. https://doi.org/10.1007/s11075-015-0087-2

[6] S. Boccaletti, J. Kurths, G. Osipov, D. L. Valladares, C. S. Zhou, *The synchronization of chaotic systems*, Physics reports, **366**(1-2) (2002), 1-101. https://doi.org/10.1016/S0370-1573(02)00137-0

[7] M. D. Buhmann, *Radial basis functions: Theory and implementations*, **12** , Cambridge University Press, 2003.

[8] T. L. Carroll, L. M. Pecora, *Synchronizing nonautonomous chaotic circuits*, IEEE Transactions on Circuits and Systems II: Analog and Digital Signal Processing, **40**(10) (1993), 646-650. https://doi.org/10.1109/82.246166

[9] G. W. Chang, C. I. Chen, Y. F. Teng, *Radial-Basis-Function-Based neural network for harmonic detection*, IEEE Transactions on Industrial Electronics, **57** (2010), 2171-2179. https://doi.org/10.1109/TIE.2009.2034681

[10] Y. Y. Chen, Y. T. Chang, B. S. Chen, *Fuzzy solutions to partial differential equations: Adaptive approach*, IEEE Transactions on Fuzzy Systems, **17**(1) (2009), 116-127. https://doi.org/10.1109/TFUZZ.2008.2005010

[11] J. Chen, C. Li, X. Yang, *Chaos synchronization of the distributed-order Lorenz system via active control and applications in chaotic masking*, International Journal of Bifurcation and Chaos, **28**(10) (2018), 1850121. https://doi.org/10.1142/S0218127418501213

[12] S. Chen, J. Lu, *Synchronization of an uncertain unified chaotic system via adaptive control*, Chaos, Solitons and Fractals, **14**(4) (2002), 643-647. https://doi.org/10.1016/S0960-0779(02)00006-1

[13] Y. Cui, H. G. Zhang, Y. Wang, W. Gao, *Adaptive control for a class of uncertain strict-feedback nonlinear systems based on a generalized fuzzy hyperbolic model*, Fuzzy Sets and Systems, **302** (2016), 52-64. https://doi.org/10.1016/j.fss.2015.11.015

[14] D. Ding, X. Qian, N. Wang, D. Liang, *Synchronization and anti-synchronization of a fractional order delayed memristor-based chaotic system using active control*, Modern Physics Letters B, **32**(14) (2018), 1850142. https://doi.org/10.1142/S0217984918501427

[15] L. G. Dominguez, R. A. Wennberg, W. Gaetz, D. Cheyne, O. C. Snead, J. L. P. Velazquez, *Enhanced synchrony in epileptiform activity local versus distant phase synchronization in generalized seizures*, Journal of Neuroscience, **25**(35) (2005), 8077-8084. https://doi.org/10.1523/JNEUROSCI.1046-05.2005

[16] A. Durdu, Y. Uyaroglu, *Comparison of synchronization of chaotic Burke-Shaw attractor with active control and integer-order and fractional-order P-C method*, Chaos, Solitons and Fractals, **164** (2022), 112646. https://doi.org/10.1016/j.chaos.2022.112646

[17] S. Effati, A. V. Kamyad, R. A. Kamyabi-Gol, *On infinite-horizon optimal control problems*, Zeitschrift für Analysis und ihre Anwendungen, **19**(1) (2000), 269-278. https://doi.org/10.4171/ZAA/950

[18] S. Effati, A. Nazemi, *A new approach for asymptotic stability of the nonlinear ordinary differential equations*, Journal of Applied Mathematics and Computing, **25** (2007), 231-244. https://doi.org/10.1007/BF02832349

[19] I. Famelis, A. Donas, G. Galanis, *Comparative study of feed forward and radial basis function neural networks for solving an environmental boundary value problem*, Results in Applied Mathematics, **16** (2022), 100344. https://doi.org/10.1016/j.rinam.2022.100344

[20] C. F. Feng, *Projective synchronization between two different time-delayed chaotic systems using active control approach*, Nonlinear Dynamics, **62**(1-2) (2010), 453-459. https://doi.org/10.1007/s11071-010-9733-3

[21] L. Glass, M. C. Mackey, *From clocks to chaos: The rhythms of life*, Princeton University Press, 1988.

[22] J. M. Gonzalez-Miranda, *Amplitude envelope synchronization in coupled chaotic oscillators*, Physical Review E, **65**(3) (2002), 036232. https://doi.org/10.1103/PhysRevE.65.036232

[23] A. Hadian Rasanan, N. Bajalan, K. Parand, J. Amani Rad, *Simulation of nonlinear fractional dynamics arising in the modeling of cognitive decision making using a new fractional neural network*, Mathematical Methods in the Applied Sciences, **43** (2020), 1-30. https://doi.org/10.1002/mma.5981

[24] M. Hajipour, A. Jajarmi, *Numerical solution of the state-delayed optimal control problems by a fast and accurate finite difference θ-method*, Communications in Nonlinear Science and Numerical Simulation, **55** (2018), 265-276. https://doi.org/10.1016/j.cnsns.2017.07.017

[25] C. Hammond, H. Bergman, P. Brown, *Pathological synchronization in Parkinsonɑs disease: Networks, models and treatments*, Trends in Neurosciencesm, **30**(7) (2007), 357-364. https://doi.org/10.1016/j.tins.2007.05.004

[26] R. Hermann, A. Krener, *Nonlinear controllability and observability*, IEEE Transactions on Automatic Control, **22**(5) (1977), 728-740. https://doi.org/10.1109/TAC.1977.1101601

[27] K. Hirosawa, S. Kittaka, Y. Oishi, F. Kannari, T. Yanagisawa, *Phase locking in a Nd: YVO 4 waveguide laser array using Talbot cavity*, Optics Express, **21**(21) (2013), 24952-24961. https://doi.org/10.1364/OE.21.024952

[28] M. C. Ho, Y. C. Hung, *Synchronization of two different systems by using generalized active control*, Physics Letters A, **301**(5-6) (2002), 424-428. https://doi.org/10.1016/S0375-9601(02)00987-8

[29] K. Hornick, M. Stinchcombe, H. White, *Multilayer feedforward networks are universal approximators*, Neural Networks, **2**(5) (1989), 359-366. https://doi.org/10.1016/0893-6080(89)90020-8

[30] L. Huang, R. Feng, M. Wang, *Synchronization of chaotic systems, via nonlinear control*, Physics Letters A, **320**(4) (2004), 271-275. https://doi.org/10.1016/j.physleta.2003.11.027

[31] L. Jianyu, L. Siwei, Q. Yingjian, H. Yaping, *Numerical solution of elliptic partial differential equation using radial basis function neural networks*, Neural Networks, **16**(5-6) (2003), 729-734. https://doi.org/10.1016/S0893-6080(03)00083-2

[32] S. Karimi, S. Effati, F. Ghane, *The synchronization of chaotic systems applying the parallel synchronization method*, Physica Scripta, **94** (2016), 1-20. https://doi.org/10.1088/1402-4896/ab2679

[33] F. Kheyrinataj, A. Nazemi, *Fractional Chebyshev functional link neural network-optimization method for solving delay fractional optimal control problems with Atangana–Baleanu derivative*, Optimal Control Applications and Methods, **41**(3) (2020), 808-832. https://doi.org/10.1002/oca.2572

[34] F. Kheyrinataj, A. Nazemi, *Muntz-Legendre neural network construction for solving delay optimal control problems of fractional order with equality and inequality constraints*, Soft Computing, **24** (2020), 9575-9594. https://doi.org/10.1007/s00500-019-04465-7

[35] R. Kiruthika, R. Krishnasamy, S. Lakshmanan, M. Prakash, A. Manivannan, *Non-fragile sampled-data control for synchronization of chaotic fractional-order delayed neural networks via LMI approach*, Chaos, Solitons and Fractals, **169** (2023), 113252. https://doi.org/10.1016/j.chaos.2023.113252

[36] S. Kopeikin, M. Efroimsky, G. Kaplan, *Relativistic celestial mechanics of the solar system*, John Wiley Sons, 2011. https://doi.org/10.1002/9783527634569

[37] M. Kumar, N. Yadav, *Multilayer perceptrons and radial basis function neural network methods for the solution of differential equations*, A Survey, Computers and Mathematics with Applications, **62** (2011), 3796-3811. https://doi.org/10.1016/j.camwa.2011.09.028

[38] C. Liu, L. Liu, T. Liu, *A novel three-dimensional autonomous chaos system*, Chaos, Solitons and Fractals, **39**(4) (2009), 1950-1958. https://doi.org/10.1016/j.chaos.2007.06.079

[39] M. Liu, W. Peng, M. Hou, Z. Tian, *Radial basis function neural network with extreme learning machine algorithm for solving ordinary differential equations*, Soft Computing, **27** (2023), 3955-3964. https://doi.org/10.21203/rs.3.rs-1416056/v1

[40] E. N. Lorenz, *Deterministic nonperiodic flow*, Journal of The Atmospheric Sciences, **20**(2) (1963), 130-141. https://doi.org/10.1175/1520-0469(1963)020<0130:DNF>2.0.CO;2

[41] N. Mai-Duy, T. Tran-Cong, *Numerical solution of differential equations using multiquadric radial basis function networks*, Neural Networks, **14**(2) (2001), 185-199. https://doi.org/10.1016/S0893-6080(00)00095-2

[42] S. Mall, S. Chakraverty, *Chebyshev neural network based model for solving Lane–Emden type equations*, Applied Mathematics and Computation, **247** (2014), 100-114. https://doi.org/10.1016/j.amc.2014.08.085

[43] S. Mall, S. Chakraverty, *Single layer Chebyshev neural network model for solving elliptic partial differential equations*, Neural Processing Letters, **45**(3) (2017), 825-840. https://doi.org/10.1007/s11063-016-9551-9

[44] M. Mansoori, A. Nazemi, *Solving infinite-horizon optimal control problems of the time-delayed systems by Haar wavelet collocation method*, Network: Computation in Neural Systems, **35** (2016), 97-117. https://doi.org/10.1080/0954898X.2021.1884762

[45] A. K. Mittal, *Error analysis and approximation of Jacobi pseudospectral method for the integer and fractional order integro-differential equation*, Applied Numerical Mathematics, **171** (2022), 249-268. https://doi.org/10.1016/j.apnum

[46] J. J. Moré, *The Levenberg-Marquardt algorithm: Implementation and theory*, In: Numerical Analysis, Springer, (1978), 105-116. https://doi.org/10.1007/BFb0067700

[47] M. Mortezaee, M. Ghovatmand, A. Nazemi, *An application of a fuzzy system for solving time delay fractional optimal control problems with Atangana–Baleanu derivative*, Optimal Control Applications and Methods, **43**(6) (2022), 1753-1777. https://doi.org/10.1002/oca.2924

[48] M. Mortezaee, M. Ghovatmand, A. Nazemi, *Solving variable-order fractional delay differential algebraic equations via fuzzy systems with application in delay optimal control problems*, Iranian Journal of Fuzzy Systems, **21**(2) (2024), 67-85. https://doi.org/10.22111/IJFS.2024.43498.7646

[49] F. Mostajeran, S. M. Hosseini, *Radial basis function neural network (RBFNN) approximation of Cauchy inverse problems of the Laplace equation*, Computers and Mathematics with Applications, **141** (2023), 129-144. https://doi.org/10.1016/j.camwa.2023.04.026

[50] U. Parlitz, L. Junge, *August synchronization of chaotic systems*, In 1999 European Control Conference (ECC) (4637-4642), IEEE, (1999). https://doi.org/10.1002/3527607455.CH11

[51] L. Perko, *Differential equations and dynamical systems*, Springer Science Business Media, **7** (2013).

[52] M. Raissi, P. Perdikarism, G. E. Karniadakis, *Physics-informed neural networks: A deep learning framework for solving forward and inverse problems involving nonlinear partial differential equations*, Journal of Computational Physics, **378** (2019), 686-707. https://doi.org/10.1016/j.jcp.2018.10.045

[53] T. Rezazadeh, E. Najafi, *Jacobi collocation method and smoothing transformation for numerical solution of neutral nonlinear weakly singular Fredholm integro-differential equations*, Applied Numerical Mathematics, **181** (2022), 135-150. https://doi.org/10.21203/rs.3.rs-4186485/v1

[54] R. Roy, Jr. K. Scott Thornburg, *Experimental synchronization of chaotic lasers*, Physical Review Letters, **72** (2009). https://doi.org/10.1103/PhysRevLett.72.2009

[55] M. G. Rosenblum, A. S. Pikovsky, J. Kurths, *Phase synchronization of chaotic oscillators*, Physical Review Letters, **76**(11) (1996), 1804. https://doi.org/10.1103/PhysRevLett.76.1804

[56] O. E. Rossler, *Continuous chaos-four prototype equations*, Annals of the New York Academy of Sciences, **316**(1) (1979), 376-392. https://doi.org/10.1111/j.1749-6632.1979.tb29482.x

[57] N. F. Rulkov, M. M. Sushchik, L. S. Tsimring, H. D. Abarbanel, *Generalized synchronization of chaos in directionally coupled chaotic systems*, Physical Review E, **51**(2) (1995), 980. https://doi.org/10.1103/PhysRevE.51.980

[58] S. J. Russell, P. Norvig, *Artificial intelligence - A modern approach*, 3rd Edition, Prentice Hall, 2010.

[59] H. Saberi-Nik, P. Rebelo, M. Shamsyeh Zahedi, *Solution of infinite horizon nonlinear optimal control problems by piecewise adomian decomposition method*, Mathematical Modelling and Analysis, **18**(4) (2013), 543-560. https://doi.org/10.3846/13926292.2013.841598

[60] F. Setoudeh, M. M. Dezhdar, M. Najafi, *Nonlinear analysis and chaos synchronization of a memristive-based chaotic system using adaptive control technique in noisy environments*, Chaos, Solitons and Fractals, **164** (2022), 112710. https://doi.org/10.1016/j.chaos.2022.112710

[61] L. Shi, X. Yang, Y. Li, Z. Feng, *Finite-time synchronization of nonidentical chaotic systems with multiple time-varying delays and bounded perturbations*, Nonlinear Dynamics, **83**(1-2) (2016), 75-87. https://doi.org/10.1007/s11071-015-2310-z

[62] G. Simone, F. C. Morabito, *RBFNN-based hole identification system in conducting plates*, IEEE Transactions on Neural Networks, **12**(6) (2001), 1445-1454. https://doi.org/10.1109/72.963779

[63] S. Singh, A. T. Azar, Q. Zhu, *Multi-switching Master Slave synchronization of nonidentical chaotic systems*, In Innovative Techniques and Applications of Modelling, Identification and Control, (321-330) (2018), Springer, Singapore.

[64] M. Srivastava, S. P. Ansari, S. K. Agrawal, S. Das, A. Y. T. Leung, *Anti-synchronization between identical and non-identical fractional-order chaotic systems using active control method*, Nonlinear Dynamics, **76**(2) (2014), 905-914. https://doi.org/10.1007/s11071-013-1177-0

[65] A. Staiano, R. Tagliaferri, W. Pedrycz, *Improving RBF networks performance in regression tasks by means of a supervised fuzzy clustering*, Neurocomputing, **69** (2006), 1570-1581. https://doi.org/10.1016/j.neucom.2005.06.014

[66] H. Su, R. Luo, M. Huang, J. Fu, *Practical fixed time active control scheme for synchronization of a class of chaotic neural systems with external disturbances*, Chaos, Solitons and Fractals, **157** (2022), 111917. https://doi.org/10.1016/j.chaos.2022.111917

[67] Z. Wang, M. Chen, J. Chen, *Solving multiscale elliptic problems by sparse radial basis function neural networks*, Journal of Computational Physics, **492** (2023), 112452. https://doi.org/10.1016/j.jcp.2023.112452

[68] L. X. Wang, J. M. Mendel, *Fuzzy basis functions, universal approximation, and orthogonal least-squares learning*, IEEE Transactions on Neural Networks, **3**(5) (1992), 807-814. https://doi.org/10.1109/72.159070

[69] Y. Wang, C. Sun, Z. Wang, J. Sun, *Projection synchronization of three-dimensional chaotic systems with active control based on DNA strand displacement*, IEEE Transactions on NanoBioscience, **22** (2023), 836-844. https://doi.org/10.1109/TNB.2023.3241652

[70] E. Wu, X. Yang, *Adaptive synchronization of coupled nonidentical chaotic systems with complex variables and stochastic perturbations*, Nonlinear Dynamics, **84**(1) (2016), 261-269. https://doi.org/10.1007/S11071-015-2433-2

[71] L. Xiao, Y. Zhang, L. Jia, Y. He, *A ZNN-based sliding mode control strategy for solving synchronization problems of chaotic systems with application in memristor oscillator*, Journal of the Franklin Institute, **360** (2023), 12101-12124. https://doi.org/10.1016/j.jfranklin.2023.09.019

[72] X. Yang, Y. Feng, K. F. C. Yiu, Q. Song, F. E. Alsaadi, *Synchronization of coupled neural networks with infinite-time distributed delays via quantized intermittent pinning control*, Nonlinear Dynamics, **94**(3) (2018), 2289-2303. https://doi.org/10.1007/s11071-018-4449-x

[73] M. Yavari, A. Nazemi, *An efficient numerical scheme for solving fractional infinite-horizon optimal control problems*, ISA Transactions, **94** (2019), 108-118. https://doi.org/10.1016/j.isatra.2019.04.016